

Review

A Review of Carbon Capture and Valorization Technologies

Jiban Podder ^{1,2}, Biswa R. Patra ², Falguni Pattnaik ² , Sonil Nanda ²  and Ajay K. Dalai ^{2,*}¹ Department of Physics, Bangladesh University of Engineering and Technology, Dhaka 1000, Bangladesh² Department of Chemical and Biological Engineering, University of Saskatchewan, Saskatoon, SK S7N 5A9, Canada* Correspondence: ajay.dalai@usask.ca; Tel.: +1-306-966-4771

Abstract: Global fossil fuel consumption has induced emissions of anthropogenic carbon dioxide (CO₂), which has emanated global warming. Significant levels of CO₂ are released continually into the atmosphere from the extraction of fossil fuels to their processing and combustion for heat and power generation including the fugitive emissions from industries and unmanaged waste management practices such as open burning of solid wastes. With an increase in the global population and the subsequent rise in energy demands and waste generation, the rate of CO₂ release is at a much faster rate than its recycling through photosynthesis or fixation, which increases its net accumulation in the atmosphere. A large amount of CO₂ is emitted into the atmosphere from various sources such as the combustion of fossil fuels in power plants, vehicles and manufacturing industries. Thus, carbon capture plays a key role in the race to achieve net zero emissions, paving a path for a decarbonized economy. To reduce the carbon footprints from industrial practices and vehicular emissions and attempt to mitigate the effects of global warming, several CO₂ capturing and valorization technologies have become increasingly important. Hence, this article gives a statistical and geographical overview of CO₂ and other greenhouse gas emissions based on source and sector. The review also describes different mechanisms involved in the capture and utilization of CO₂ such as pre-combustion, post-combustion, oxy-fuels technologies, direct air capture, chemical looping combustion and gasification, ionic liquids, biological CO₂ fixation and geological CO₂ capture. The article also discusses the utilization of captured CO₂ for value-added products such as clean energy, chemicals and materials (carbonates and polycarbonates and supercritical fluids). This article also highlights certain global industries involved in progressing some promising CO₂ capture and utilization techniques.



Citation: Podder, J.; Patra, B.R.; Pattnaik, F.; Nanda, S.; Dalai, A.K. A Review of Carbon Capture and Valorization Technologies. *Energies* **2023**, *16*, 2589. <https://doi.org/10.3390/en16062589>

Academic Editor: Alberto Maria Gambelli

Received: 9 February 2023

Revised: 5 March 2023

Accepted: 7 March 2023

Published: 9 March 2023



Copyright: © 2023 by the authors. Licensee MDPI, Basel, Switzerland. This article is an open access article distributed under the terms and conditions of the Creative Commons Attribution (CC BY) license (<https://creativecommons.org/licenses/by/4.0/>).

Keywords: carbon dioxide; fossil fuels; greenhouse gas; sequestration; storage; utilization

1. Introduction

The reduction in carbon emissions and the advancement of carbon capture technology is a global demand for sustainable human health and the environment. To maintain a healthy environment and better human life, mitigation of greenhouse gas (GHGs) emissions is essential. The emissions and concentrations of GHGs such as carbon dioxide (CO₂), methane (CH₄), nitrous oxide (N₂O), ozone (O₃) and water vapor are increasing in the environment day by day due to rapid urbanization and industrialization. Recently, the subject of carbon capture, its mechanism and utilization have become an important issue and a global challenge. The increasing everyday demand for electricity and fuels for vehicles and industries is met by the combustion of fossil fuels, especially petroleum, natural gas and coal. The extraction, upgrading and utilization of fossil fuels contribute to the emission of CO₂, which lead to global warming and climate change [1]. GHGs result from both natural processes (e.g., decomposition of organic matter, forest fires, volcanic eruptions, etc.) and human activities (e.g., fossil fuels extraction and utilization, industrial manufacturing, incineration, deforestation, changes in land management and forestry practices, livestock farming and agriculture) [2,3]. With a total worldwide emission rate of 40 gigatons/year and nearly 3200 gigatons in the atmosphere, CO₂ is the most predominant

GHG. The highest CO₂ exchange (i.e., 440 gigatons per annum) occurs between the land and atmosphere through photosynthesis [4].

Among conventional fossil fuels, coal is the main source of energy for power generation, and it is the second-largest feedstock of primary energy after crude oil [5]. Out of the total energy demand, 84% of energy is derived from fossil fuels (including 33%, 24% and 27% from oil, natural gas and coal, respectively) followed by 6% from hydroelectricity, 4% from nuclear power and 5% from renewable sources [6]. To overcome this crucial challenge, renewable energy sources such as solar, wind, tidal and nuclear power can play a big role in reducing carbon emissions and maximizing clean power generation.

Figure 1 shows the increase in CO₂ concentration over the years. For example, the current CO₂ level of 418.3 ppm is 23% higher than that of 1980 (i.e., 339.6 ppm) [7]. Recent studies have shown that humans emit more than 565 gigatons of CO₂ each year through anthropogenic activities [8]. This causes the earth's temperature to increase through the greenhouse effect and global warming. Figure 2 illustrates the global average temperature anomaly from 1850 to 2020. It can be noticed that the global average temperature has risen sharply over the years above 1.1 °C [9]. This increase in global temperature can cause catastrophic environmental and ecological impacts such as (i) severe weather conditions (e.g., heat waves, hurricanes, floods and wildfires); (ii) an increase in sea levels; (iii) acidity of oceans; (iv) decreasing groundwater levels and drought; (v) shortage of drinking water; (vi) loss of arable land area; (vii) compromised agriculture, aquaculture and livestock farming; (viii) soil erosion; (ix) outbreak of insects and pests; (x) adverse effects to human and animal health; (xi) poor quality of water, air and soil; and (xii) risks to infrastructures, artifact and monuments [10].

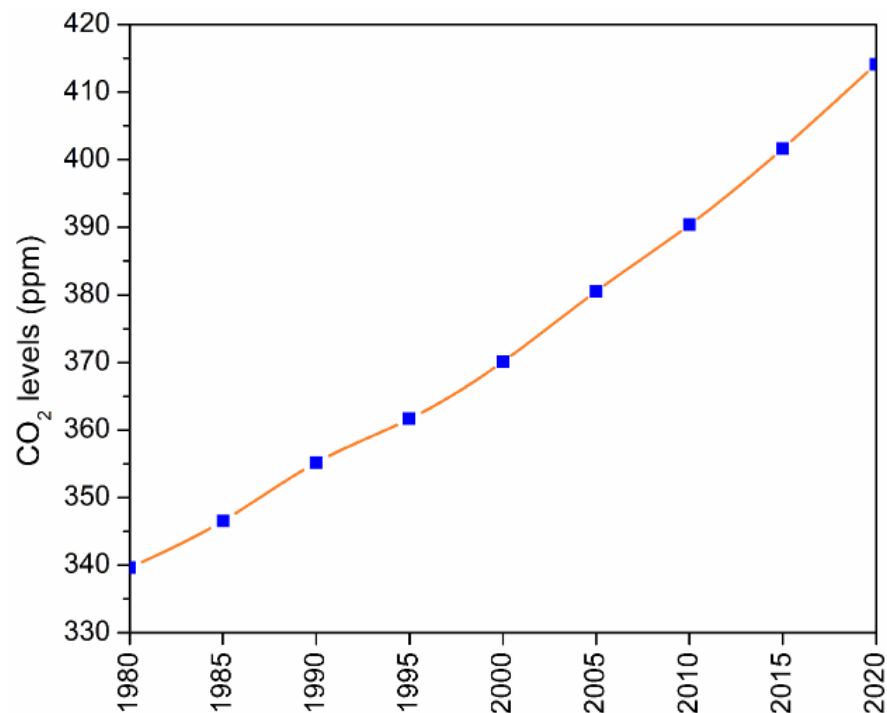


Figure 1. Global atmospheric CO₂ concentrations (Data source: [7]).

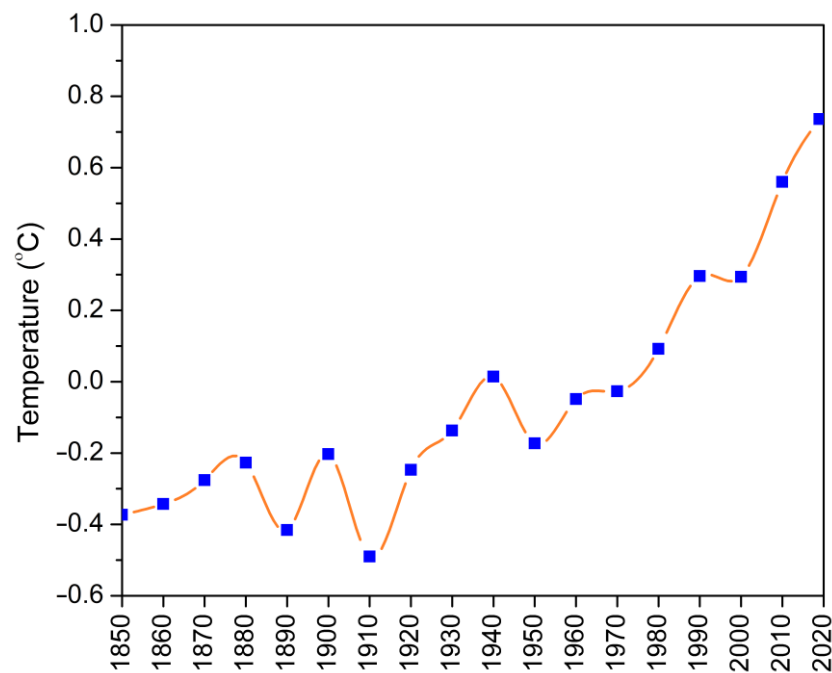


Figure 2. Global average temperature anomaly (Data source: [9]).

These adversities have given overwhelming realization to the science community, legislators and humanity on the potential of CO₂ emission reduction and capturing approaches to prevent the catastrophic effects of anthropogenic climate change. The carbon capture and storage strategies have been considered one of the prime choices for reducing the CO₂ levels in the atmosphere [11]. Considering the global consciousness of this issue, in 2021, the United Nations Climate Change Conference (or the Conference of the Parties, COP26) in Glasgow proposed to keep down the global temperature below 1.5 °C and to reach net-zero emission of carbon by 2050 [12]. To achieve these targets, it is important to phase out the utilization of coal, prevent deforestation, switch to electric vehicles and deploy renewable fuels as alternative energy sources. As an outcome of this COP26 Glasgow Climate Pact, out of 197 participating countries, 140 countries vowed to reach net-zero emissions, 100 countries pledged to reverse deforestation, 40 countries agreed to phase out coal and 24 countries showed commitment to accelerate the sales and use of electric vehicles.

Several research studies have been conducted on CO₂ capture, utilization and storage technologies. This article reports some recent studies on carbon and GHG emissions and an in-depth discussion of the recent advances in carbon capture, utilization and storage technologies. We have made a rigorous attempt to identify the knowledge gaps and comprehensively review the literature that is foundational, most recent and relevant to carbon capture and sequestration technologies. To develop this comprehensive review, a theory- and evidence-based methodology has been adopted to advance the knowledge of CO₂ capturing and valorization pathways by summarizing quantitative information and providing recommendations for future inquiry.

2. Greenhouse Gas Emissions

GHG emissions have resulted from different sources such as the energy sector, industry, landfill, buildings, transport, agriculture, forestry and other land uses. Some common GHGs include CO₂, CH₄, N₂O, O₃, water vapor and fluorinated gases (FG). As illustrated in Figure 3, the current atmospheric concentration of GHGs, especially CO₂, CH₄, N₂O and FG are 76%, 16%, 6% and 2%, respectively [13]. Different GHGs persist in the environment or the atmosphere for longer durations due to their different absorption capacities and lifetimes in the atmosphere. An excess of trapping heat ultimately increases the earth's temperature and eventually changes the climate, as discussed earlier. GHGs cover the

earth’s atmosphere as an insulating layer, which warms this planet by trapping heat energy and increasing the global temperature. The emission of CO₂ into the atmosphere is through anthropogenic and natural sources. Anthropogenic sources of CO₂ emission are mostly through human activities such as the extraction, processing and combustion of fossil fuels, deforestation and industrial manufacturing. The natural sources of CO₂ emissions are volcanic eruptions, ocean outgassing, decomposition of organic matter and wildfires [14].

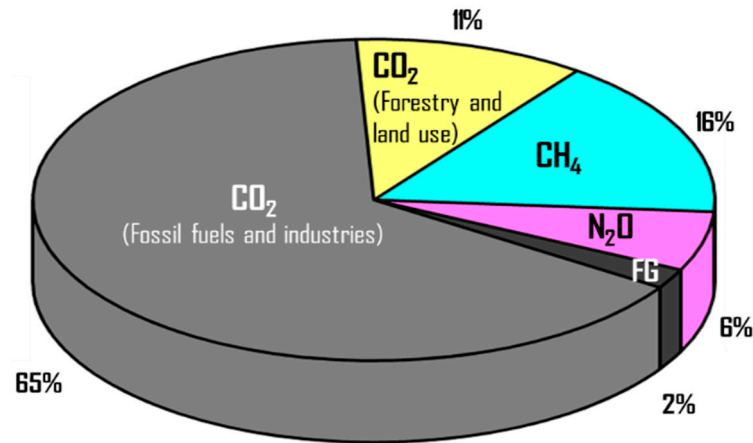


Figure 3. Global atmospheric concentrations of greenhouse gases (Data source: [13]).

As shown in Figure 4, the current primary sources of GHG emissions are heat and power generation (25%), followed by agriculture, forestry and land use (24%), industries (21%), transportation (14%), other energy industries (10%) and building exhausts (6%) [13]. The burning of fossil fuels for power generation, oil refining and various industrial and transportation activities induce an unprecedented increase in global CO₂ emissions. Among the various types of fossil fuels, coal releases the prime amount of CO₂. Approximately 40% of CO₂ released into the atmosphere is attributed to coal combustion in 2021 [15].

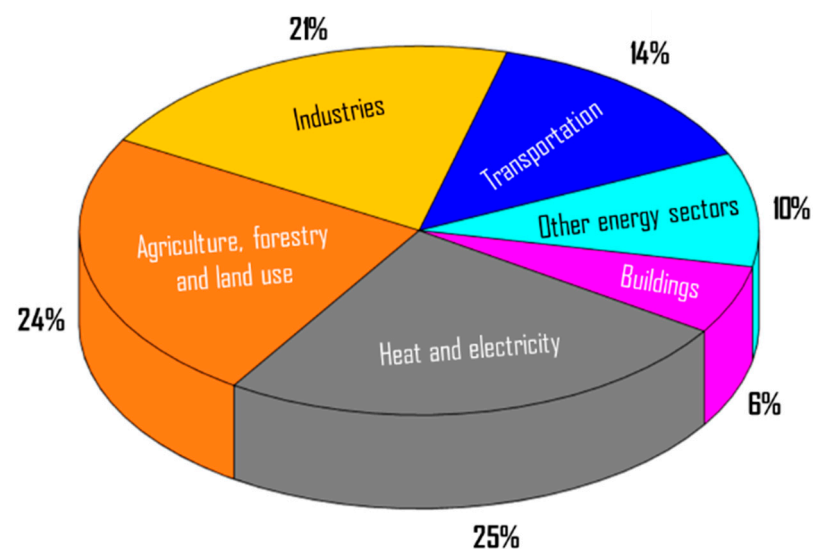


Figure 4. Global greenhouse gas emissions by sectors (Data source: [13]).

Most commonly, there are four major industrial processes through which a great deal of CO₂ emissions takes place such as cement production, iron and steel production, chemicals production and extraction of fossil fuels, and petrochemical products. Among the major industrial processes, steel-making and cement production release a significant amount of CO₂. Limestone (CaCO₃) is the main source of cement production. When limestone is

heated at a high temperature, calcium oxide (CaO) and a large amount of CO₂ are released as byproducts of the chemical reaction. During the production of 1 ton of cement, roughly 0.95 tons of CO₂ is released [16]. Similarly, in the steel and iron industry, when the iron is melted and purified to reduce its carbon content, contact with oxygen releases CO₂. For every ton of steel manufactured, 1.9 tons of CO₂ is released, accounting for 6.7% of global GHG emissions [17]. In the petrochemical industry, CO₂ is released for manufacturing products such as refined oil, plastics, solvents and lubricants. Furthermore, CO₂ emission is linked to the point source where carbon is being used as feedstock in calcination, a reducing agent for the manufacturing of metal and the fermentation of biomass [18].

To understand the global warming impacts of different GHGs, the global warming potential (GWP) unit is used. GWP measures the ability to trap the heat of each GHG in the atmosphere compared to CO₂ over a specified period. The period is typically considered 100 years for GWPs. GWP is measured as the amount of heat energy absorbed by any GHG in the atmosphere as a multiple of the heat that would be absorbed by the same mass of CO₂. In the unit, GWP is equal to one for CO₂ as the reference of standard gas regardless of the period used. The larger the value of GWP, the warmer the earth is compared to CO₂ over that period. CO₂ remains in the atmosphere for quite a very long time, causing it to increase its concentrations to last for thousands of years. N₂O remains in for an average of 114 years in the atmosphere. In the atmosphere, N₂O has 298 times the impact on an equal amount of CO₂ for 100 years. Various industrial processes, refrigeration products and consumer products contribute to different fluorinated gases such as hydrofluorocarbons (HFCs), hydrochlorofluorocarbons (HCFCs), chlorofluorocarbons (CFCs), perfluorocarbons (PFCs), sulfur hexafluoride (SF₆) and nitrogen trifluoride (NF₃). These gases have a high-GWP value in the thousands or tens of thousands as they can trap more heat than CO₂. CH₄ is considered to have a GWP of 28–36 above 100 years. In the atmosphere, the lifetime of CH₄ is much shorter than CO₂, but it can trap more heat than CO₂.

CH₄ is released from the decomposition of organic matter by methanogenic bacteria and the burning of fossil fuels including coal and heavy oil. CH₄ has 25 times more impact than CO₂ on global warming and climate change. The production of CH₄ from the decomposition of organic matter through anaerobic digestion is influenced by organic matter composition, oxygen deficiency, temperature, moisture and decomposition time. Im et al. [19] studied the impact of storage temperatures ranging from 15 °C to 35 °C on solid cattle manure and found that the highest emission of CH₄ was recorded at a temperature of 35 °C.

Aerosols have an impact on climate change. Aerosols are suspended in the atmosphere as dust particles for a short period instead of quickly falling to the surface. Aerosols originate from natural sources such as volcanoes, marine plankton and the burning of fossil fuels and biomass. Upon the reflection of sunlight, aerosols have a cooling effect and the absorption of sunlight has a warming effect. Aerosols react with clouds and can contribute to both cooling and warming effects by reflecting sunlight or by trapping heat.

3. Carbon Capture Technologies

CO₂ capture technologies are of global importance because CO₂ emissions from fossil fuels have significantly threatened the economy, the environment, natural ecosystems and human health. Advances in carbon capture and utilization technology can dramatically reduce CO₂ emissions and lead the path towards net zero and achieve several United Nations Sustainable Development Goals, especially Goal 6 (Clean Water and Sanitation), Goal 7 (Affordable and Clean Energy), Goal 9 (Industry, Innovation and Infrastructure), Goal 11 (Sustainable Cities and Communities), Goal 12 (Responsible Consumption and Production) and Goal 13 (Climate Action).

Carbon capture, storage and utilization can be achieved in four phases. The first step is the removal of CO₂ from the point source. Flue gases are emitted from industrial plants and are considered the point source through physical and chemical absorption, adsorption, membrane-based separation and other emerging technologies [20,21]. Compressed CO₂ in

liquid form is easy to store and transport. CO₂ can be stored permanently underground by injecting it into porous rocks or under ocean beds through geo-sequestration [22]. The selection of locations depends on the abundance of porous rock in the ground. The injected CO₂ fills out the pores inside the rocks and is detained there from above by covering an impermeable layer. This technique is very similar to the storage phenomenon of oil and gas underground. Both onshore and offshore basins can be used for the geological storage of CO₂. The utilization of captured CO₂ is intended to convert the captured CO₂ into valuable chemicals, enhance oil recovery and recover untapped oil or alkaline remediation. The combusted exhaust gas is used as the feedstock material for utilization. CO₂ is used in food and beverage processing and for producing synthetic or hydrocarbon fuels in combination with hydrogen.

Figure 5 illustrates the main pathways for CO₂ capture and utilization. The main methods for CO₂ capture are pre-combustion, post-combustion, oxyfuel combustion and direct air capture. The available technologies for CO₂ capture are adsorption, membrane separation, chemical looping, cryogenic distillation and hydrate-based separation. The captured CO₂ can be utilized to produce clean fuels, chemicals and valuable minerals, enhanced oil recovery and other direct uses. Table 1 summarizes the principles and promising aspects of some CO₂ utilization technologies.

3.1. Pre-Combustion

Figure 6 graphically represents the interconnected mechanisms of pre-combustion, post-combustion, oxy-fuel combustion and other industrial CO₂ capture processes [27]. Pre-combustion takes place before the combustion process where the fuel is gasified in the presence of oxygen and steam, resulting in syngas production. CO present in the syngas is converted into CO₂ through the water–gas shift reaction and captured before combustion, whereas H₂ present in the syngas is used as a direct fuel in the gas turbines [28]. The pre-combustion capture technique uses both physical and chemical methods to capture CO₂ from processed syngas. Chemical absorbents such as carbonates and physical solvents such as methanol and polypropylene glycol are generally used for CO₂ capture on a commercial scale [29]. The pre-combustion route can proportionately reduce costs by 38–45% and 21–24% compared to the post-combustion and oxy-combustion routes [30]. However, owing to the modernization of existing facilities, an additional cost is involved regarding the setup of the process units such as gasifiers and water–gas shift reactors, which limits commercialization.

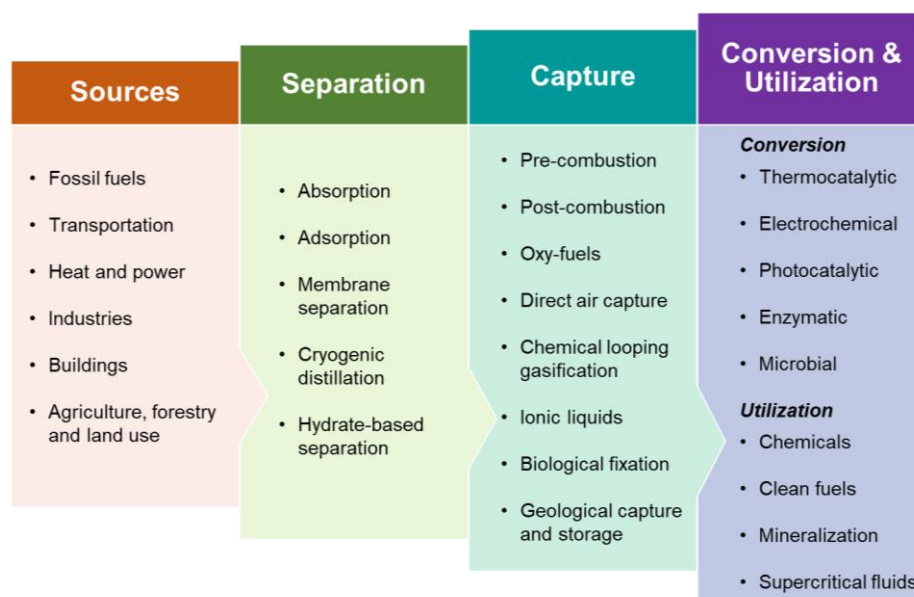


Figure 5. Common routes for CO₂ separation, capture and utilization.

Table 1. Summary of CO₂ utilization processes.

Pathway	Principle	Benefits
Biochar production	Waste biomass (agricultural, woody, algal and municipal solid waste) can be thermochemically and hydrothermally carbonized to produce biochar.	<ul style="list-style-type: none"> • Biochar locks the carbon for use as a fuel, soil amendment agent and adsorbent to remove pollutants from wastewater and CO₂ from flue gases. • Biochar can replace coal and reduce GHGs. • CO₂ can be sequestered for centuries in the form of biochar.
Algae cultivation	Algae utilize CO ₂ directly from the atmosphere for photosynthesis.	<ul style="list-style-type: none"> • Harvesting and processing algae can produce biofuels, proteins, lipids, bioactive compounds, biochar and activated carbon for diverse industrial and environmental applications. • CO₂ released from the utilization of biofuels can be recycled by algae and plants for photosynthesis to make the process carbon neutral. • In addition to biologically fixing CO₂, algae can treat wastewater and industrial flue gases.
Production of building materials	CO ₂ can be mineralized into carbonates and limestones.	<ul style="list-style-type: none"> • Production of bricks, concrete and other construction materials. • The captured CO₂ in the form of construction materials can be stored for centuries.
Enhanced oil recovery	Injection of captured CO ₂ into oil reservoirs along with water.	<ul style="list-style-type: none"> • Enhances oil production substantially. • The chances of releasing CO₂ are comparatively low.
Chemicals production	CO ₂ captured from industrial flue gases and the atmosphere can be converted into valuable chemicals.	<ul style="list-style-type: none"> • Chemicals such as methanol, dimethyl ether, ethylene, formic acid, urea and bioplastic building blocks can be produced. • Biochemicals can fetch a higher market value than petrochemicals.
Clean fuel production	CO ₂ captured from industrial flue gases and the atmosphere can be converted into valuable biofuels.	<ul style="list-style-type: none"> • Clean fuels such as methanol, dimethyl ether and Fischer-Tropsch-derived hydrocarbon fuels (i.e., green diesel, jet fuels, ethanol and butanol) can be produced. • Biorefineries can earn carbon credits by recycling CO₂ to produce clean fuels.

References: Aresta et al. [23]; Shafawi et al. [24]; Zhang and Liu [25]; Valluri et al. [26].

Dakota Gasification Company's Great Plains Synfuels Plant in North Dakota, USA, produces 150 million ft³ of syngas from the gasification of about 18,000 tons of lignite coal [31]. The company also implements the methanol-based Rectisol process at an annual capacity of 3 mt-CO₂ [32]. About 155 million ft³ of CO₂ is compressed and sent to a Canadian oil field in Weyburn-Midale fields located in southeastern Saskatchewan via a 320 km pipeline for enhanced oil recovery [33,34]. Mississippi Power's Kemper County energy facility intended to perform gasification of lignite coal and store its captured carbon emissions pre-combustion of the syngas. However, the project was shelved in 2017 due to project delays and increased costs [35]. According to the literature, although there are some pilot-scale studies of pre-combustion carbon capture, there is a lack of full-scale pre-combustion facilities at a global scale [32].

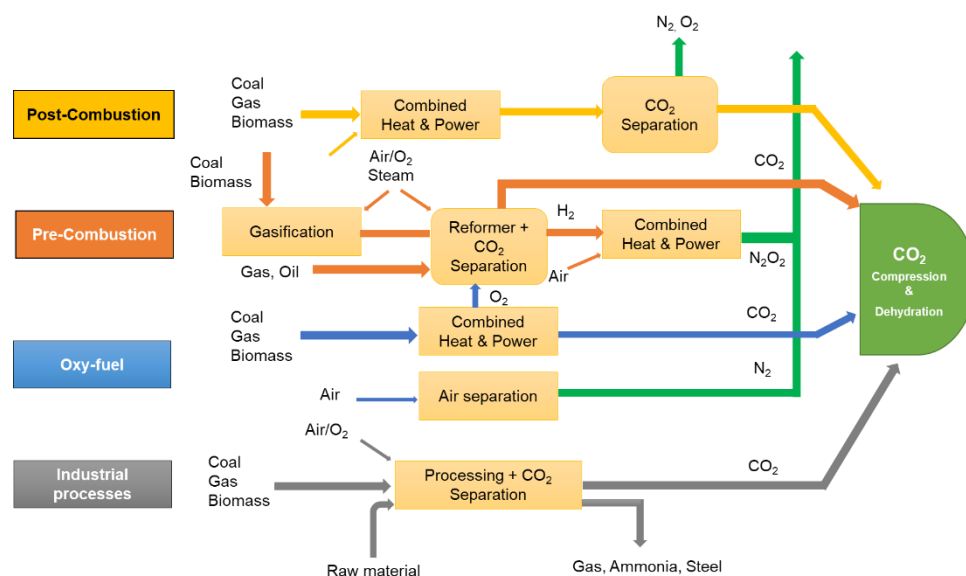


Figure 6. Graphical illustration of post-combustion, pre-combustion and oxy-fuel carbon capture technologies (Adapted from IPCC [27]).

3.2. Post-Combustion and Oxy-Fuel Technologies

In the post-combustion technique, CO_2 is removed after the combustion process from the flue gas released from coal-fired power plants and other manufacturing industries. The post-combustion technologies are the favored option for modifying existing power plants. The most common pathways in post-combustion carbon capture are membrane separation, chemical absorption, chemical looping and physical adsorption. Examples of industries implementing post-combustion carbon capture, especially amine-based processes, include Mitsubishi Heavy Industries Ltd. (Tokyo, Japan), HTC Purenergy (Canada), Aker Carbon Capture (Norway) and Kerr-McGee/ABB Lummus (USA) [32]. AES Warrior Run Power Plant in Maryland, USA, generates over 180 MW of energy from coal, and 4–6% of the captured CO_2 (via amine-based adsorption process) is sold to food and beverage industries [36]. Linde has partnered with BASF in implementing post-combustion carbon capture and using amine as a solvent to scrub CO_2 from the flue gas stream [37]. Linde's post-combustion carbon capture plant in Wilsonville, USA, can process $9100 \text{ Nm}^3/\text{h}$ of flue gas and capture 42 tons/day of CO_2 [38]. Similarly, Linde's post-combustion carbon capture plant in Niederaussem, Germany, processes $1552 \text{ Nm}^3/\text{h}$ of flue gas and captures 7.2 tons/day of CO_2 [38]. Recently, ExxonMobil has announced its partnership with National Renewable Energy Laboratory (NREL) and National Energy Technology Laboratory (NETL) to advance its collaboration in research and development relating to biofuels, process intensification, life-cycle assessment and carbon capture [39].

The oxy-fuel technique is like the post-combustion process, except that the fuel is fired in the presence of oxygen. It makes the flue gas more concentrated with CO_2 , which enhances its capturing process [29]. Using an oxy-fuel boiler, the Linde/BASF plant in Schwarze Pumpe, Germany, can capture 240 tons/day of CO_2 from a $7000 \text{ Nm}^3/\text{h}$ flue gas stream [38]. NET Power LLC in the USA has successfully demonstrated a low-cost and emission-free oxy-fuel combustion facility in La Porte, Texas, which is a 50 MW natural gas power plant and the only large-scale supercritical CO_2 -based plant in the world [40].

3.3. Direct Air Capture

In the air, CO_2 is found in a much lighter form than that found in industrial flue gases. Currently, there are two approaches to removing CO_2 from the air such as solid and liquid direct air capture (DAC). Solid DAC technology uses solid sorbent materials which can hold CO_2 by chemical adsorption. The stored concentrated CO_2 in the filter can be recovered by heating or keeping it in a vacuum system for further storage or use. In

the liquid DAC systems, the air is passed through a solution of hydroxide, which strips the CO₂. The captured CO₂ can then be stored in the deep geological rocks or ocean beds by injection under high pressure [41]. Although the DAC process is expensive, there are some benefits of the DAC process such as a lower land and water requirement and a low bulk transportation cost of captured CO₂. The cost of operation depends on the bestowing technology approach, whether the CO₂ will be stored geologically or be cast off directly under low pressure.

Strong bases or aqueous hydroxide solutions such as KOH and NaOH are used as solvents to chemisorb CO₂ for DAC technologies [42]. The chemisorbed CO₂ is then converted into carbonates and bicarbonates. Monoethanolamine is an aqueous amine solvent that is found effective for scrubbing flue gas by interacting with CO₂ and converting it into carbamate anions that could later hydrolyze to bicarbonate [43]. One of the main challenges encountered in amine-solvent-based DAC is the loss of solvent due to evaporation as large volumes of air or flue gases are blown over the aqueous solution and potential amine degradation over the longer reaction period [44]. Some mitigation strategies include the following: (i) using less volatile amine solvents or amine derivatives such as amino acids [45] and (ii) using porous solid supports such as silica, organic polymers and metal-organic frameworks to immobilize reactive amine groups [46]. It has also been reported that higher concentrations of amine can lower energy consumption and equipment size, thereby reducing the operating expenditure of the carbon sequestration process [32].

Although the DAC process is relatively expensive, it has some major benefits such as a lower land and water requirement and a low bulk transportation cost of captured CO₂. The cost of operation depends on the technology approach, i.e., whether CO₂ will be stored geologically or cast off directly under low pressure. Freitas et al. [47] demonstrated a conceptual nano-factory-based molecular filter powered by solar energy at a low cost of U.S. \$18.3/ton of CO₂. In another study by Kiani et al. [48], the projected cost for DAC captured CO₂ per ton was estimated to be U.S. \$114 at a scale of 1 MtCO₂ per year.

Climeworks AG, a Switzerland-based company, is one of the world's first commercial DAC plants [49]. The design uses an adsorption-desorption process on alkaline-functionalized adsorbents. The adsorption of CO₂ takes place at ambient conditions while the temperature-vacuum swing process is used for desorption. It also uses an amine-supported cellulose fiber-based filter to adsorb CO₂ molecules. Produced CO₂ in this process is >99.8% pure, and simultaneously H₂O is released as a byproduct [50]. In 2017, the plant was able to capture 900 tons of CO₂ per annum. The technology requires 2000 kWh of energy per ton of CO₂, and the capture process is powered by renewable energy sources. The cost of CO₂ removal and permanent storage via mineralization is expected to be less than U.S. \$100/ton of CO₂ over the years [51]. Furthermore, Carbon Engineering in British Columbia, Canada, uses high-temperature aqueous solutions for DAC [52]. Global Thermostat in Colorado, USA is a DAC company, which can remove CO₂ from the atmosphere at the point source emissions [53].

3.4. Chemical Looping Combustion and Gasification

In the first approach, limestone (CaCO₃) can be taken as sorbents to preserve CO₂ from the gas mixture. When solid CaCO₃ is heat treated at around 850 °C to 950 °C in a calciner, it decomposes into gaseous CO₂ and solid CaO. The pure stream of CO₂ is then collected and purified for storage or use. In another approach, CO₂ can be seized through the liquid solvent or other separation methods. Under the absorption-based approach, once the CO₂ is captured by the solvent, then CO₂ can be removed in high-purity form by heating. This technology is widely used in capturing CO₂ for use in the food and beverage industry. Strong bases aqueous solution of soda lime, NaOH, KOH and LiOH can remove CO₂ by chemical reaction. LiOH was used in the canister of the spacecraft of the historic manned lunar landing mission, Apollo 11 in 1969, to remove CO₂ from the atmosphere [54].

Clean H₂ can be produced by applying oxidation and reduction-based chemical looping technology [55]. In this technology, coal or syngas-based chemical looping systems

use looping particles of metal in contact with oxygen from the combustion air to form metal oxide. There are two steps of separation taking place in two fuel reactors. In the first step, the oxidation of fossil fuels such as coal or biomass is accomplished, and in the second step, gas separation is performed to produce high-purity H₂. The exodus stream contains CO₂ along with water after condensing out pure CO₂. The advantage of this technique is that it does not require cleaning up the fuel gas before separating H₂. In addition, at high pressure, the chemical looping system produces a stream of CO₂ which eliminates a costly pressurization step.

Owing to the properties of electrophilicity in carbon atoms, organic–inorganic bases with strong nucleophilic atoms can be extensively used in capturing CO₂. Hence, the bases interact directly with CO₂ as a proton acceptor. The harvested CO₂ could be used for the synthesis of valuable chemicals. Pure and high-pressure CO₂ is needed in most processes of CO₂ conversion to value-added fuels, chemicals and products manufacturing.

Chemical looping combustion and gasification is emerging as a new method for CO₂ capture during fuel processing; it also has some limitations that impede scaling up. Some of the bottlenecks are the following: (i) high endothermicity of combustion and gasification; (ii) high cost of oxygen required for largescale combustion and gasification; (iii) operating expenditures for maintenance of combustion and gasification reactors when dealing with heterogeneous feedstocks; (iv) agglomeration, sintering, low lifetime and high cost of applied catalysts; (v) sensitivity of operating conditions and (vi) limited choices for oxygen carriers [56]. To address these issues, in situ gasification chemical looping combustion has emerged [57]. In this new approach, the fuel emissions such as CO₂ and H₂O are recirculated to play as gasifying agents. Hence, the volatile vapors and syngas generated from gasification are oxidized in a gas–solid reaction in the presence of an oxygen carrier.

3.5. Ionic Liquids

In recent advances, ionic liquids have opened a new avenue in capturing CO₂ with a high capacity [58]. Ionic liquids have unique characteristics such as low vapor pressures, high thermal stability, high solubility of CO₂ as well as tunable properties [59,60]. The active sites of the ionic liquids are responsible for the capture of CO₂ through chemical absorption. Furthermore, the ionic liquid can act as an activator for CO₂ conversion as well [61]. Oxazolidinones, cyclocarbonates, quinazoline-2,4-(1H,3H)-diones organic ionic liquids are prepared for CO₂ absorbents and as catalysts [62]. Some other functionalized ionic liquids such as amino-acid-based [63],azole-based [64] and phenol-based ionic liquids [65] with improved properties were developed. In addition, aqueous amine solutions such as mono-ethanolamine (MEA) and methyl-di-ethylamine (MDEA) are also found to be promising in entrapping CO₂ [66].

Luo et al. [67] have extensively studied CO₂ capture using ionic liquids. In their experiment, bi-functionalized ionic liquids were used in capturing and instantaneously fixing CO₂ to recurring carbonates. Hence, the cation can arrest CO₂, whereas the anion can actuate the substrate to promote CO₂ infusion. The yield of the product can be improved in addition to a small amount of water and may be more applicable to industrial exhaust. The disadvantage of this technique is the low absorption kinetics of CO₂ due to the relatively high viscosity of the ionic liquid [68]. Moreover, the disadvantages are high volatility, expensive, intense energy utilization and corrosiveness and the great importance is the selection of the solvents.

The use of an ionic liquid has facilitated the transformation of CO₂ as rich products via the chemical, biochemical, photochemical, thermochemical and electrochemical reduction approaches [69]. Among the various approaches, the chemical and electrochemical mechanisms have become promising for the reduction of CO₂. In the chemical process, epoxides and methanol solvents are used to convert CO₂ to carbonates and cyclic through cycloaddition reactions, separately. The electrochemical reduction method is becoming a more probable mechanism as of its high efficiency, high conversion capability, storing of electrical energy and production quality from a renewable source such as solar energy [70].

3.6. Biological CO₂ Fixation

Several studies have reported the benefits of elevated CO₂ in inducing the productivity of certain crops such as paddy and wheat [71–73]. Greater CO₂ concentration in the atmosphere can increase the rate of photosynthesis in plants leading to the elevated synthesis of carbohydrates in plants, thus increasing the biomass yield. On the other hand, single-celled algae are the smallest form of plants that reproduce at a rapid rate compared to terrestrial plants [74]. Furthermore, algae can tolerate extreme environmental conditions with high proliferation rates, fix CO₂ into carbohydrates and lipids and grow in wastewater, thus treating pollution [75,76]. CO₂ plays a vital role in algal growth since the biomass formed in algal cells as lipids and proteins can be further converted into valuable fuels, chemicals, bioactive compounds, nutraceuticals, pharmaceuticals and cosmeceuticals [77].

The biological conversion of CO₂ using microalgae is another route of carbon capture and fixation [78]. This mechanism involves the absorption of CO₂ by algae through photosynthesis. Microalgae can be cultivated in open ponds and photobioreactors to potentially produce biofuels and nutraceuticals, carbon sequestration and treat wastewater [79]. Microalgae contain significant levels of lipids or triglycerides, which can be transformed into biodiesel by the transesterification process. Biofuels are considered carbon neutral because the emitted CO₂ after their combustion is utilized by plants and algae for photosynthesis, thus leading to CO₂ fixation [80,81].

The research with flue gas has shown tolerance of microalgae *Scenedesmus obliquus* to the high concentration of CO₂ and toxic metals [82]. Microalgae can capture CO₂ from the atmosphere and industrial flue gas, and can also fix CO₂ in the form of soluble carbonates [75]. A study by Chou et al. [83] reported high carbon assimilation rates of 272 and 194 mg/L/day by microalgae *Chlorella vulgaris* ESP-31 mutant strains 283 and 359, respectively. Moreover, algae-based biochar also finds application in carbon sequestration, feedstock for activated carbon production and adsorption of toxic compounds from polluted air, water and soil [84–86].

3.7. Geological CO₂ Capture and Storage

Geological sequestration is an effective process for capturing CO₂ from the source point at industries or a related energy source and storing it in deep geological formations such as depleted oil and gas reservoirs, coal beds and deep saline formations [87–89]. Geological CO₂ sequestration consists of three important stages such as CO₂ capture, transportation and storage. In the capture stage, the CO₂ is separated from other gases at the point source of emissions using different technologies. The captured CO₂ is compressed into dense fluid and transported via pipelines or ships to the storage location. In the final stage, the compressed CO₂ is injected into the deep geological formations to store it permanently.

Bulk transportation of CO₂ is primarily performed in high-pressure and compressed form through pipelines that can stretch for several thousands of kilometers. For bulk transportation, CO₂ is typically converted to its supercritical fluid state by increasing its temperature and pressure above the critical points, i.e., 31 °C and 7.4 MPa. The transportation of CO₂ in its supercritical fluid form through pipelines is considered economical compared to transportation in the gaseous form [90]. Safety is of primary importance for environmental assessment while transporting highly dense CO₂ under high pressures in pipelines. A leakage or accidental release of CO₂ during transportation may occur by the failure of the construction materials due to corrosion, rupture, puncture, defects in welding, ground movement and/or operator errors [90].

Geological storage of CO₂ is performed mostly in the depleted oil and gas reservoirs through injection under high-pressure, compressed and fluidized form (supercritical CO₂) to displace the remaining oil and gas. The pressure of the reservoir ranges from 4.4 to 110 MPa [91]. The other feasible geological formations for CO₂ storage are saline formations located in highly permeable and porous sedimentary basins with the largest storage capacity [88]. The saline formations have an estimated CO₂ storage capacity of 400–100,000 Gt [92,93]. The CO₂ trapping mechanism is a key factor in geological CO₂

sequestration, which includes hydrodynamic trapping, structural, residual, solubility, adsorption and mineral trapping [94]. Another geological CO₂ sequestration technique is coal seam-based sequestration. Coal seams are naturally occurring geological formations containing coal and methane. The concept of methane displacement from coal seams with the injection of CO₂, which can be stored in coal, forms the basis of this technique. The field application in coal seam-based CO₂ sequestration has been implemented quite often.

Geological sequestration is a rapidly developing field with ongoing research and development efforts toward addressing economic, technical and environmental challenges. A risk management strategy is generally used to avoid the risks involved during CO₂ injection and post-injection storage at the storage site. In San Juan, USA, from 1995 to 2001, 336,000 tons of CO₂ was injected to recover methane, which increased from 77% to 95% [95]. Furthermore, in the Qinshui basin in Shanxi, China, in 2010, CO₂ injection (234 tons) resulted in a 2.5-fold increase in CH₄ production [96]. The In Salah CO₂ storage project in Algeria, started in 2004, has injected and stored more than 3.8 MT of CO₂ in the subsurface [97]. The Sleipner CO₂ storage project in Norway started in 1996 and stored CO₂ in a deep saline reservoir 800–1000 m below the seabed with an annual capacity of 0.9 MT [98].

4. Conversion of CO₂ into Value-Added Products

The recent trends in CO₂ utilization technologies have advanced significantly and shifted towards the fuel synthesis, production of carbonates, polycarbonates and different valuable chemicals such as formic acid, formaldehyde, methane, syngas, ethanol, methanol, dimethyl ether, urea and salicylic acid [18,99]. Solar fuel involves the conversion of solar or other renewables to chemical energy; thus, a chemical energy carrier is produced. Fuels with high energy density make them apposite for energy storage and transportation. CO₂ utilization has evolved as a suitable carbon-based solar fuel without distorting the existing infrastructures. The process involves the splitting of CO₂ into CO and O₂. CO can be processed with green H₂ to produce a wide range of clean fuels and chemicals via the Fischer–Tropsch process [100].

4.1. Conversion of CO₂ into Chemicals and Clean Fuels

Most refineries require syngas, hydrogen, aromatics, ethanol, alkanes (i.e., methane and ethane) and light olefins (ethylene) to produce several industrial chemicals and clean fuels. Such materials are generally fossil-based, and to permanently restrict the dependency on fossil fuels, switching to clean fuels and chemicals and combined utilization of CO₂ is inevitable [101]. CO₂ is considered a potential feedstock for the synthesis of several chemicals such as olefins, methanol, isopropanol, formic acid, acetaldehyde and formaldehyde. There are several methods such as thermocatalytic [102–111], electrochemical [112–116], photocatalytic [117–122], enzymatic [123] and microbial [124,125] techniques available for CO₂ conversion to fine chemicals, as summarized in Table 2. Due to significant research and development, the thermocatalytic CO₂ conversion to chemicals and fuels is the most popular route for large-scale industrial applications. Hydrogenation [126,127], methanation [128], dry reforming [129], reverse water-gas shift reaction [130] and Fischer–Tropsch synthesis [131] are some of the thermocatalytic processes involving homogeneous and heterogeneous catalysts for CO₂ conversion into clean fuels and chemicals.

Perathoner and Centi [131] extensively studied the application of CO₂ along with H₂ to produce light olefins via catalytic Fischer–Tropsch synthesis. In addition to the thermochemical conversion of CO₂ via the Fischer–Tropsch process, microbial conversion of CO₂ is also reported. Liu et al. [107] demonstrated an energy-efficient CO₂ hydrogenation to clean fuels and chemicals by employing reactive separations of CO/CO₂ mixtures. The applications are extended to the U.S. Navy's seawater-to-fuel process. The authors applied a Ru–Co single atom alloy catalyst for Fischer–Tropsch synthesis to generate C₅₊ hydrocarbons at a productivity of 11.7 μmol/s/g-Co from a 50:50 CO/CO₂ gas stream at 200 °C and a high gas hourly space velocity (GHSV) of 84,000 mL/g/h. The relatively low

process temperature and high GHSV were compatible with the upstream reverse water–gas shift reaction. The study inferred that ruthenium dopants promoted the reduction in Co species, thus enhancing CO hydrogenation without playing major roles in improving desired C₅₊ hydrocarbon selectivity via Fischer–Tropsch synthesis.

Table 2. Summary of promising studies on the conversion of CO₂ into chemicals and clean fuels.

Conversion Method	Main Process Specifications	Main Products	Reference
Thermocatalytic	<ul style="list-style-type: none"> Feedstock: CO₂ with 34.5 mmol epoxides (propylene oxide) Reactor: 50 mL stainless-steel autoclave Catalyst: Zn(Py) (Atz) Co-catalyst of Bu₄NBr Catalyst loading: 0.1 g Co-catalyst loading: 0.1 g Temperature: 100 °C Pressure: 1.5 MPa Time: 4 h 	<ul style="list-style-type: none"> Propylene carbonate yield: 92.1% Selectivity: 99% 	Lan et al. [102]
Thermocatalytic	<ul style="list-style-type: none"> Feedstock: CO₂:H₂ = 1:3 CO₂ flow rate: 10 mL/min H₂ flow rate: 30 mL/min Ar: 5 mL/min Gas hourly space velocity: 13,500 mL/h/g(cat) Reactor: CO₂ hydrogenation reactor Catalyst: 5 wt.% Fe/H-ZSM-5 Catalyst loading: 0.2 g Temperature: 335 °C Pressure: 2.1 MPa Time on stream: 12 h 	<ul style="list-style-type: none"> CO₂ conversion: 5.7% CH₄ selectivity: 28.4% CO selectivity: 60.9% C₂–C₄ alkanes selectivity: 9.7% Olefins: 0.7 mL/h/g(cat) 	Liu et al. [103]
Thermocatalytic	<ul style="list-style-type: none"> Feedstock: CO₂:H₂ = 1:3 CO₂ flow rate: 10 mL/min H₂ flow rate: 30 mL/min Ar: 5 mL/min Weight hourly space velocity: 36 L/h/g(cat) Reactor: Stainless steel reactor with 6.35 mm diameter Catalyst: 0.8 wt.% K/Co (5 wt.%)-ZSM-5 (Si/Al: 100) Temperature: 300 °C Pressure: 2.2 MPa Time on stream: 12 h 	<ul style="list-style-type: none"> CO₂ conversion: 25.4% CH₄ selectivity: 57.9% CO selectivity: 17.3% C₂–C₄ alkanes selectivity: 20.8% C₅₊ selectivity: 3.9% 	Liu et al. [104]
Thermocatalytic	<ul style="list-style-type: none"> Feedstock: CO₂:H₂ = 1:3 Weight hourly space velocity: 1.5–150 mL/s/g(cat) Reactor: Packed bed reactor Catalyst: Mo₂C/SiO₂ Temperature: 300 °C Pressure: 2.1 MPa 	<ul style="list-style-type: none"> CO₂ conversion: 9% CH₄ selectivity: 12.9% CO selectivity: 82.7% C₂₊ selectivity: 4.4% Ethane yield: 3.1% Ethylene yield: 0.2% Propane yield: 0.7% Propene yield: 0.3% Butane yield: 0.1% CO yield: 7.5% [production rate: 22.2 μmol CO/g(cat)/s] 	Juneau et al. [105]

Table 2. Cont.

Conversion Method	Main Process Specifications	Main Products	Reference
Thermocatalytic	<ul style="list-style-type: none"> • Feedstock: CO₂:H₂ = 1:3 • CO₂ flow rate: 10 mL/min • H₂ flow rate: 30 mL/min and • Ar: 5 mL/min • Gas hourly space velocity: 27,000 mL/h/g(cat) • Reactor: Packed bed reactor (diameter: 0.25 in and length: 12 in) • Catalyst: W_xC nanoparticle calcined at 1000 °C • Catalyst loading: 0.1 g • Temperature: 350 °C • Pressure: 2.1 MPa • Time on stream: 12 h 	<ul style="list-style-type: none"> • CO₂ conversion: 13.9% • CH₄ selectivity: 5% • CO selectivity: 94.6% • C₂-C₄ selectivity: 0.4% • CO yield: 13.1% • O₂ uptake: 2.7 μmol/g 	Juneau et al. [106]
Thermocatalytic	<ul style="list-style-type: none"> • Feedstock: CO₂:H₂ = 1:2.5 • CO₂ flow rate: 2 mL/min • CO flow rate: 2 mL/min • H₂ flow rate: 10 mL/min • Ar: 4 mL/min • Gas hourly space velocity: 5000 mL/h/g(cat) • Reactor: Stainless steel reactor (Outer diameter: 6.35 mm, inter diameter: 4.57 mm and length: 40 mm) • Catalyst: Ru-Co single atom alloy: Boron nitride (1:5) • Catalyst loading: 168 mg • Temperature: 200 °C • Pressure: 300 psig • Time on stream: 12 h 	<ul style="list-style-type: none"> • CO₂ conversion: 4.4% • CO conversion: 16.4% • CH₄ selectivity: 22.7% • C₂-C₄ alkenes selectivity: 17.2% • C₂-C₄ alkanes selectivity: 14.2% • C₅₊ selectivity: 46% 	Liu et al. [107]
Thermocatalytic	<ul style="list-style-type: none"> • Feedstock: CO₂/H₂ (3:1) • Catalyst: 0.5% CuO/ZnO-ZrO₂ • Catalyst loading: 0.2 g catalyst with 0.4 g of quartz • Temperature: 290 °C • Pressure: 4.5 MPa • Time: 2 h 	<ul style="list-style-type: none"> • CO₂ conversion: 9.5% • Methanol yield: 7.2% 	Xu et al. [108]
Thermocatalytic	<ul style="list-style-type: none"> • Feedstock: CO₂ and propylene oxide • Reactor: 50 mL autoclave • Catalyst: Zn (dobdc) (datz)/Bu₄NBr • Catalyst loading: 0.16 mmol (Zn) • Co-catalyst loading: 0.46 mmol (Bu₄NBr) • Temperature: 80 °C • Time: 7 h • Pressure: 1.5 MPa 	<ul style="list-style-type: none"> • Propylene carbonate yield: 98% 	Lan et al. [109]
Thermocatalytic	<ul style="list-style-type: none"> • Feedstock: CO₂:H₂O = 1:1 • CO₂ flow rate: 0.2 L/min • H₂O flow rate: 0.2 L/min • Reactor: Catalytic reactor • Catalyst: Ni/Mn/Ru-TiO₂ nanorods • Temperature: 425 °C 	<ul style="list-style-type: none"> • Methanol yield: 8 wt.% • Methanol production rate: 2 mmol/g/h 	Krishnan and Jakka [110]

Table 2. Cont.

Conversion Method	Main Process Specifications	Main Products	Reference
Thermocatalytic	<ul style="list-style-type: none"> • Feedstock: CO₂:H₂ = 1:1 • Reactor: 300 mL stainless steel batch reactor • Catalyst: 4.7 wt.% Ru-CO₃O₄ • Catalyst loading: 0.2 g • Temperature: 120 °C • Time: 6 h • Pressure: 6.2 MPa 	<ul style="list-style-type: none"> • Formic acid yield: 310 mmol 	Bankar et al. [111]
Electrochemical	<ul style="list-style-type: none"> • Feedstock: CO₂ in the cathode (flow rate: 20 mL/min) • Reference electrode: Ag/AgCl electrode • Working electrode: Silver foil • Reference electrode: Platinum foil • Electrolyte: 0.1 M KHCO₃ 	<ul style="list-style-type: none"> • Faradaic efficiency of H₂: around 100% (at cell potential of −0.6 V) • Faradaic efficiency of CO: 90% (at cell potential of −1 V) • Faradaic efficiency of formate: 10% (at cell potential of −1.3 V) 	Hatsukade et al. [112]
Electrochemical	<ul style="list-style-type: none"> • Feedstock: CO₂ in the cathode (flow rate: 20 mL/min) • Anode: Graphite-nano IrO₂ on gas diffusion electrode • Cathode: Nano tin on gas diffusion electrode with polystyrene vinylbenzyl methyl imidazolium chloride • Membrane: Nafion 212 (anode) and Sustainion X37-50 (cathode) • Time: 500 h 	<ul style="list-style-type: none"> • Formic acid concentration: 15–18% • Faradaic efficiency at a cell voltage of 3.3–3.4: 30% 	Yang et al. [113]
Electrochemical	<ul style="list-style-type: none"> • Feedstock: CO₂ in the cathode (flow rate: 20 mL/min) • H-type electrolytic cell • Nafion 117 membrane • Reference electrode: Ag/AgCl • Counter electrode: Pt sheet • Working electrode: Glass electrode (Nafion + Cu₂O@Cu-MOF) • Electrolyte: 0.1 M KHCO₃ 	<ul style="list-style-type: none"> • Faradaic efficiency of ethylene: 79.4% • Faradaic efficiency of CH₄: 63.2% 	Tan et al. [114]
Electrochemical	<ul style="list-style-type: none"> • Feedstock: CO₂ in the cathode • Reactor: Two-compartment electrochemical cell • Electrocatalyst: Zn-Cu alloy • Electrolyte: 0.1 M KHCO₃ 	<ul style="list-style-type: none"> • Faradaic efficiency of CO: 97.3% (at cell potential of −0.96 V) • H₂: 15.26% (at cell potential of −1.05 V) • Formate: 4.27% (at cell potential of −1.05 V) 	Wang et al. [115]
Electrochemical	<ul style="list-style-type: none"> • Feedstock: CO₂ in the cathode (flow rate: 10 mL/min) • Reactor: Three-electrode H-type electrochemical cell • Reference electrode: Ag/AgCl • Counter electrode: Pt electrode • Working electrode: Cu₇₆In₂₄ hydroxides • Electrolyte: 0.1 M KHCO₃ 	<ul style="list-style-type: none"> • Faradaic efficiency of CO: 75.8% (at cell potential of −0.59 V) • Faradaic efficiency of H₂: 70% (at cell potential of −1.2 V) • Faradaic efficiency of formate: 85% (at cell potential of −1.01 V) 	Xie et al. [116]

Table 2. Cont.

Conversion Method	Main Process Specifications	Main Products	Reference
Electrochemical	<ul style="list-style-type: none"> • Feedstock: CO₂ in the cathode (flow rate: 20 mL/min) • CHI760e electrochemical workstation (H-type electrolytic cell) • Nafion 117 membrane • Reference electrode: Ag/AgCl • Counter electrode: Pt sheet • Working electrode: glass electrode (Nafion + 4 mg Pd₃Ag alloys) • Electrolyte: 0.1 M KHCO₃ 	<ul style="list-style-type: none"> • Faradaic efficiency of formic acid at 0.03 V: 69% • Faradaic efficiency at 0.2 V: 96% 	Yang et al. [113]
Photocatalytic	<ul style="list-style-type: none"> • Feedstock: gas phase CO₂ • Light source: Xenon arc lamp • Photocatalyst: C₃N₄/SnS₂ • Catalyst loading: 0.5 g • Temperature: Ambient • Pressure: Ambient 	<ul style="list-style-type: none"> • Methane • Methanol 	Di et al. [117]
Photocatalytic	<ul style="list-style-type: none"> • Feedstock: CO₂ • Light source: Halogen lamp • Photocatalyst: Carbon-doped tin sulfide • Catalyst loading: 0.1 g 	<ul style="list-style-type: none"> • Acetaldehyde (CH₃CHO) 	Shown et al. [118]
Photocatalytic	<ul style="list-style-type: none"> • Feedstock: Liquid CO₂ • Light source: White LED light • Photocatalyst: rGO/CuZnO/Fe₃O₄ • Catalyst loading: 0.1 g • Reaction medium: H₂O/dimethylformamide: 5:45 	<ul style="list-style-type: none"> • Methanol 	Kumar et al. [119]
Photocatalytic	<ul style="list-style-type: none"> • Feedstock: CO₂ (400 ppm) with 0.5 mL water (reducing agent) • Light source: 500 W Xenon lamp • Photocatalyst: Molybdenum doped WO₃ • Catalyst loading: 25 mg 	<ul style="list-style-type: none"> • Methane yield: 5.3 μmol/g/h 	Wang et al. [120]
Photocatalytic	<ul style="list-style-type: none"> • Feedstock: CO₂ with H₂O as reducing agent • Light source: 300 W Xenon lamp (λ: 320–780 nm) • Photocatalyst: CuO_n/ZnO • Catalyst loading: 5 mg 	<ul style="list-style-type: none"> • Ethane yield: 2.7 μmol/g/h (32.9%) • Methane yield: 2.2 μmol/g/h (26.9%) • CO: 3.3 μmol/g/h (32.9%) 	Wang et al. [121]
Photocatalytic	<ul style="list-style-type: none"> • Feedstock: CO₂ with sodium bicarbonate (0.1 M) as the reducing agent • Light source: 350 W Xenon lamp • Photocatalyst: TiO₂-MoS_xSe_y • Temperature: Ambient • CO₂ pressure: 0.2 MPa 	<ul style="list-style-type: none"> • Ethanol yield: 704 μmol/g/h 	Long et al. [122]

Table 2. Cont.

Conversion Method	Main Process Specifications	Main Products	Reference
Enzymatic	<ul style="list-style-type: none"> • Feedstock: CO₂ with 2.2 mmol/L NADH (nicotinamide adenine dinucleotide + hydrogen) • Biobased catalyst: Enzymes (carbonic anhydrase, formate dehydrogenase and glutamate dehydrogenase) immobilized on HKUST-1@amine-MIL-101(Cr) • Catalyst loading: 30 mg • Temperature: 25 °C • Pressure: 0.5 MPa • Time: 6 h 	<ul style="list-style-type: none"> • CO₂ conversion: 71.1% • Formic acid yield: 4–5 mmol/L 	Li et al. [123]
Microbial	<ul style="list-style-type: none"> • Feedstock: CO₂ • Microbial strain: <i>Synechococcus elongates</i> 	<ul style="list-style-type: none"> • Isopropanol yield: 26.5 mg/L 	Kusakabe et al. [124]
Microbial	<ul style="list-style-type: none"> • Feedstock: CO₂ (5%) • Microbial strain: <i>Synechocystis</i> sp. (PCC6803) (efe gene overexpressed <i>Pseudomonas syringae</i>) • Temperature: 30 °C 	<ul style="list-style-type: none"> • Ethylene yield: 718 µg/L/h 	Xiong et al. [125]

Liu et al. [103] investigated the hydrogenation of CO₂ and its correlation with Fischer–Tropsch catalysis using over Fe/Na-ZSM-5 catalyst. Compared to Fe/H-ZSM-5, Fe/Na-ZSM-5 demonstrated higher catalytic stability and selectivity for olefins due to greater surface basicity and generation of active Fe₅C₂ phases. Olefins also resulted from the catalytic cracking of long-chain hydrocarbons in the presence of acidic ZSM-5 zeolite support. Owing to the greater binding strength of CO₂, Fe/Na-ZSM-5 exhibited higher selectivity towards CO. Moreover, the reverse water–gas shift reaction promoted CO₂ hydrogenation. The study suggested that attenuating the acidic properties of the catalyst could direct the selectivity to olefins and CO for Fischer–Tropsch synthesis and reverse water–gas shift reaction, respectively.

Xie et al. [132] synthesized and applied a multi-metallic catalyst (Co/Mn/Na/S) for application in Fischer–Tropsch synthesis to produce lower olefins from natural gas also containing CO₂. The promoted Co-based catalyst showed negligible activity toward the water–gas shift reaction. A 54% selectivity was obtained for olefins in the range of C₂–C₄ at 240 °C and 0.1 MPa. As the pressure increased to 1 MPa, the selectivities towards fuels and lower olefins and fuels approached 59% and 30%, respectively. The authors proposed that a synergistic effect between Na and S acted as an electronic promoter for Co, which improved selectivities towards fuels and lower olefins while significantly lowering the yields of CO₂ and CH₄.

One of the main challenges in Fischer–Tropsch synthesis is the low selectivity towards certain light olefins when CO is replaced with CO₂ in the syngas feedstock. To further investigate this challenge, Liu et al. [104] synthesized and applied different potassium-promoted Co/ZSM-5 catalysts for selective hydrogenation of CO and CO₂. The authors reported that with a tunable Si/Al ratio in the support and potassium promoters for Co-based catalysts, the selectivity towards light olefins can be significantly improved in Fischer–Tropsch synthesis using both CO and CO₂ as the feedstocks.

Owing to their high catalytic activity and adjustable selectivity towards C₁ products, transition metal carbides have shown many promises in the conversion of CO₂ [Juneau et al., 2022]. Juneau et al. [105] studied the effects of acidity of the catalyst support as a factor for reverse water–gas shift reaction. Significant variations were

observed in CO production rates of 1.3 μmol and 22.2 $\mu\text{mol CO}/\text{min}/\text{g}$ over silicalite-1 and SiO_2 , respectively. The authors reported that by altering the physicochemical and surface properties of Mo_2C -based support (i.e., amorphous $\gamma\text{-Al}_2\text{O}_3$ and SiO_2), the performance and product selectivity of reverse water-gas shift reaction can be controlled. The variation in support material also enables a more facile reduction in Mo to an oxy-carbide state to favor the performance of reverse water-gas shift reaction. The oxidation state and catalytic activity of Mo are also influenced by the physicochemical and surface properties of the catalyst support combined with the Lewis acidity of the catalyst [106].

Martín and Grossmann [133] utilized CO_2 captured from the gasification of switchgrass to produce methanol where the required H_2 was sourced from the electrolysis of water. In a catalytic CO_2 reforming process, Xu et al. [108] reported a methanol yield of 7.2% from CO_2/H_2 using 0.5% CuO doped Zn-Zr mixed oxide at 290 °C under 4.5 MPa pressure in 2 h. In another study, a higher methanol yield was reported using Ni/Mn/Ru-TiO₂ nanorods from the conservation of CO_2 in presence of water at 425 °C [110]. Several recent studies have also reported on the photocatalytic and microbial conversion of CO_2 into ethanol and butanol, which are considered superior fuels and platform chemicals [122,134].

Renewable energy harnessed from solar, tidal or wind can be used for the electrochemical reduction of CO_2 . Hatsukade et al. [112] studied the electrochemical reduction in CO_2 on metallic silver surfaces under ambient conditions to produce chemicals such as formate, methanol and ethanol along with CH_4 . The authors reported that a silver-based catalyst resulted in a C-C coupled product during the electrochemical reduction in CO_2 .

Morales-Guio et al. [135] developed and applied an electrocatalyst composed of gold nanoparticles on a polycrystalline copper foil (Au/Cu) for the electrochemical reduction in CO_2 to higher alcohols. The novel Au/Cu electrocatalyst exhibited dramatic selectivity for the formation of products with C-C bonds such as C_{2+} alcohols and hydrocarbons, even at low overpotentials. The transport modeling studies suggested that a greater concentration of CO was generated upon CO_2 reduction on the bimetallic Au/Cu catalyst, which further reduced to alcohols such as ethanol and n-propanol under alkalinity. The work by Wang et al. [115] also demonstrated the synergistic effects of a bimetallic Zn/Cu catalyst synthesized via a facile galvanic-exchange synthesis procedure in promoting the electrochemical reduction in CO_2 under moderate overpotentials.

Xie et al. [116] synthesized and applied copper-indium hydroxides ($\text{Cu}_x\text{In}_y\text{-OH}$) as promising noble metal-free electrocatalysts for the electrochemical reduction of CO_2 . The authors reported that with the increase in the loading of In in the electrocatalyst, the product selectivity shifted from CO to formate, with a Faradaic efficiency of 85% at -0.01 V. On the other hand, with the increased loading of Cu in the electrocatalyst, the product selectivity was mostly towards CO achieving a Faradaic efficiency of 76% at -0.59 V.

The study by Shown et al. [118] focused on the aqueous phase photocatalytic conversion of CO_2 into acetaldehyde using carbon-doped SnS_2 in a 300 mL stainless steel vessel using a halogen lamp as the light source. In another study, Kumar et al. [119] performed photocatalytic conversion of liquid CO_2 into methanol using graphene-oxide-doped trioxide (rGO/CuZnO/ Fe_3O_4) as the potential photocatalyst in the biphasic reaction medium (i.e., water/dimethylformamide ratio of 5:45) and using white LED light as the light source. The photocatalytic conversion of CO_2 in the presence of water is ascribed to the electron-hole mechanism, which is generated by the impact of photo energy on the photocatalysts, and these free electrons and holes sensitized the photocatalytic reduction reaction of CO_2 [118].

The utilization of CO_2 in electrochemical reduction or heterogeneous catalysis of CO_2 and H_2 results in the production of formic acid [136]. Other gaseous fuels such as methane and ethane are also reported to be produced from CO_2 through hydrogenation using catalytic or photocatalytic reforming. In a catalytic study, Bankar et al. [111] synthesized ruthenium-doped Co_3O_4 to produce formic acid (HCOOH), and its highest yield was found to be 250 mmol with 0.2 g of 2.9 wt.% of catalyst loading by taking CO_2/H_2 (1:1) as the feedstock at 120 °C, 6.2 MPa pressure in 6 h. In a study by Yang et al. [137], an electrolytic

cell was designed with a graphite nano-IrO modified gas diffusion electrode as the anode and nano tin and polystyrene vinyl benzyl methyl imidazolium chloride modified gas diffusion electrode as the cathode. In this electrolytic cell, CO₂ was purged in the cathode compartment with a flow rate of 20 mL/min, which continuously produced formic acid at a concentration of 15–18% with a Faradaic efficiency of 30% at a cell voltage of 3.3–3.4 V for 500 h. Wang et al. [121] photocatalytically converted CO₂ using water as a co-feedstock and reducing agent into methane, ethane and CO using Cu-Zn mixed oxide, with a yield of 27% (2.2 μmol/g/h), 33% (2.7 μmol/g/h) and 33% (3.3 μmol/g/h), respectively. In another study, Wang et al. [120] revealed a higher selectivity and production rate of methane (5.3 μmol/g/h) with the implementation of a molybdenum-doped WO₃ catalyst.

Microbial conversion of CO₂ is also popularly implemented due to the lower product degradation during the low-temperature microbial conversion. A study by Kusakabe et al. [124] involved the microbial fermentation of CO₂ into iso-propanol with a yield of 26.5 mg/L using genetically engineered *Synechococcus elongatus*. Alcohols and aldehydes along with different carboxylic acids such as formic acid are used as platform chemicals directly as a commodity or feedstock for the making of various liquid and gaseous fuels. Xiong et al. [125] used a genetically modified *Synechocystis* species where the ethylene-forming enzyme or Efe gene of *Pseudomonas syringae* was overexpressed to convert CO₂ to ethylene at a production rate of 718 μg/L/OD/h.

4.2. Conversion of CO₂ into Organic Carbonates and Polycarbonates

Organic carbonates are considered for various useful industrial applications. A green polar solvent is used in lithium-ion batteries as electrolytes and to produce pharmaceuticals and polymeric compounds [138]. Chaugule et al. [138] presented the latest findings on the transformation of CO₂ into organic carbonates under low temperatures and pressure using ionic liquids. CO₂ storage as calcium and magnesium carbonate minerals is considered one of the efficient geological storage methods. The production of Ca or Mg carbonates involves the reaction of CO₂ with minerals such as calcium or magnesium silicates (e.g., olivine, CaSiO₃ and Mg₂SiO₄). Carbonates have many valuable industrial applications, which depend on various physicochemical properties such as particle size, shape, color, brightness, density or polymorphs of CaCO₃. CaCO₃ exists in nature in phases such as calcite, vaterite and aragonite. The formation of each polymorph is influenced by temperature, pH, composition (i.e., carbonate and calcium ions), the presence of additives, stirring and reaction time [139].

CO₂ mineralization can accelerate the large-scale industrial production of carbonates with no net energy requirement, as the carbonation reactions are all exothermic processes. Furthermore, the released heat energy during the process can be used for other thermal activities. The carbonation process also involves the treatment of solid waste, which stabilizes the toxic compounds. The applications of such treated solid waste material are in the construction industry [140]. Currently, commercial polycarbonate production utilizes phosgene. Phosgene is a highly toxic chemical and negatively impacts both the environment and human health. The phosgene can be effectively replaced by CO₂ to manufacture non-phosgene polycarbonates [141].

Lan et al. [102] reported a bi-catalytic conversion of CO₂ and propylene oxide (epoxide) into propylene carbonate with a yield of 92% using Zn(Py) (Atz) and Bu₄NBr at 100 °C under 1.5 MPa pressure in 4 h. In a similar study, an increased yield of propylene carbonate (98%) was obtained with a zinc-based catalyst i.e., Zn (dobdc) (datz) along with BU₄NBr at 80 °C under 1.5 MPa, respectively, in 7 h. Propylene carbonate, as a high boiling point polar solvent, is used in dyeing and textile industries, lithium-ion batteries and petrochemical industries for the removal of H₂S and CO₂ from fuel gases and the synthesis of different polymers such as polypropylene carbonate and polyurethane [142]. There are several industrial applications of PPC in increasing the toughness of various types of soft polymers such as epoxy resin due to its impact resistance.

4.3. Conversion of CO₂ into Supercritical Fluids

Another crucial usage of CO₂ is the conversion of CO₂ into a supercritical fluid, which can be used as an environmentally friendly medium for the extraction of various bioactive natural products. CO₂ is converted to its supercritical state, i.e., supercritical CO₂ (SCCO₂), by enhancing the temperature and pressure above its critical points, i.e., 31.1 °C and 7.4 MPa, respectively [143]. SCCO₂ is considered a promising supercritical fluid owing to its low reaction conditions, non-flammability and inexpensive nature [144]. Moreover, CO₂ in its supercritical state is almost double the density of steam. Hence, the high density and volumetric heat capacity of SCCO₂ make high heat energy operate the turbines while subsequently reducing the capital cost compared to other fluids [145]. Supercritical CO₂ behaves as a non-polar fluid-based solvent for the extraction of various non-polar and semi-polar compounds from natural resources.

The popularity of SCCO₂ is exponentially increasing due to several advantages such as the following: (i) better mass transfer due to enhanced infusibility; (ii) greater selectivity unlike other extraction media; (iii) reusability of CO₂; and (iv) solvent-free extraction and easier product recovery [146,147]. Due to the low-cost and abundance of CO₂ combined with high efficiency, low energy requirement, easy handling and tunable processing conditions, SCCO₂ technology is an appealing approach to recycling. SCCO₂ is a multipurpose solvent that has found several industrial applications such as the decaffeination of coffee beans, extraction of cannabinoids, removal of pesticides from harvested crops, dry cleaning of garments, strengthening of cement, enhanced oil recovery, upgrading of crude oil and foaming of polymers [148]. It should be noted that traditional technologies applied to each of these aspects require either a large amount of chemical solvents or petrochemicals that release toxic residues into the environment including GHGs.

SCCO₂ can also serve as a solvent and reagent in the electrochemical CO₂ reduction to address several challenges such as low solubility of CO₂ in water, mass transfer limitations hindering the transport of solutes to the electrode surface, product separation and purification, lower selectivity of products, low current densities and high over-potentials [149–151]. SCCO₂ is also explored for enhanced oil recovery [152,153] and upgrading of heavy oil [154]. It can be a cleaner alternative to fracking, steam reforming and hydrotreating technologies, which use fossil fuels and emit a substantial amount of CO₂ and GHGs. Based on the versatility of SCCO₂, several industries such as NET Power in LaPorte, Texas, USA, [155] and Air Liquide in partnership with the USA-based company Fusion Coolant Systems [156] have announced their approach to providing a breakthrough innovation for fuel processing and machinery industries to adapt SCCO₂ in their infrastructures to enhance productivity and sustainability.

One of the most recognized applications of SCCO₂ is found in the pharmaceutical, nutraceutical and cosmeceutical industries for the extraction of value-added products for consumer applications. Another benefit of SCCO₂ is the tailoring of its polarity at different pressures and temperatures, which allows for extracting bioactive compounds such as cannabinoids, tocopherol, terpenoids and fatty acids [146,157]. SCCO₂ is widely implemented to extract flavors, essential oils and different types of aromatic plants such as sandalwood, lemongrass, cannabis, rosemary, peppermint, etc. Table 3 summarizes some notable studies on SCCO₂ extraction of value-added bioactive compounds.

SCCO₂ extraction of different cannabinoids for medicinal and recreational uses is applied for its increased selectivity and purity towards certain vital cannabinoid molecules such as cannabidiol, tetrahydrocannabinol and tetrahydrocannabivarin. Pattnaik et al. [146] performed valorization of *Cannabis indica* leaves through SCCO₂ extraction and reported a cannabis oil yield of 4.9 wt.% at optimized pressure, temperature and extraction time of 25 MPa, 43 °C and 1.7 h, respectively.

Table 3. Summary of notable studies on the extraction of natural products using SCCO₂.

Feedstock	Process Parameters	Key Outcomes	Reference
Algae (<i>Nannochloropsis</i> sp.)	<ul style="list-style-type: none"> • CO₂ pressure: 55 MPa • Temperature: 75 °C • Time: 100 min • Flow rate: 14.5 g/min 	<ul style="list-style-type: none"> • Eicosapentaenoic acid: 5.6 mg/g 	Leone et al. [158]
Algae (<i>Nannochloropsis</i> sp.)	<ul style="list-style-type: none"> • CO₂ pressure: 40 MPa • Temperature: 50 °C • Time: 100 min • Flow rate: 14.5 g/min 	<ul style="list-style-type: none"> • Docosahexaenoic acid: 0.12 mg/g 	Leone et al. [158]
Almond	<ul style="list-style-type: none"> • CO₂ pressure: 40 MPa • Temperature: 60 °C • Time: 120 min 	<ul style="list-style-type: none"> • Almond oil yield: 40 wt.% 	Salinas et al. [159]
<i>Cannabis indica</i>	<ul style="list-style-type: none"> • CO₂ pressure: 25 MPa • Temperature: 43 °C • Time: 1.7 h • Flow rate: 35 g/min 	<ul style="list-style-type: none"> • <i>Cannabis</i> oil yield: 4.9 wt.% (cannabidiol: 29%, tetrahydrocannabinol: 35%, tetrahydrocannabivarin: 8%, α-humulene: 3 %, and <i>cis</i>-caryophyllene: 5 %) 	Pattnaik et al. [146]
Cherry seed	<ul style="list-style-type: none"> • CO₂ pressure: 35 MPa • Temperature: 70 °C • Time: 4 h • Flow rate: 0.4 kg/h • Particle size: <800 μm 	<ul style="list-style-type: none"> • Cherry seed oil: 13 wt.% (oleic acid: 41%, linoleic acid: 47.4% and tocopherol: 36.2%) 	Dimić et al. [160]
Clarified butter	<ul style="list-style-type: none"> • CO₂ pressure: 7 MPa • Temperature: 10 °C • Time: 60 min 	<ul style="list-style-type: none"> • Total yield: 5.9 wt.% (δ-dodecalctone: 217 ng/g, δ-tetradecalctone: 110 ng/g and 3-ethyl-3-methyl heptane: 64.8 ng/g) 	Duhan et al. [161]
Frog (<i>Rana chensinensis</i>) ovum	<ul style="list-style-type: none"> • CO₂ pressure: 29 MPa • Temperature: 50 °C • Time: 132 min • Flow rate: 80 L/h 	<ul style="list-style-type: none"> • Ovum oil yield: 13.3 wt.% (i.e., linoleic acid, oleic acid, docosahexaenoic acid, eicosapentaenoic, linolenic acid, arachidonic acid) 	Gan et al. [162]
Ginger	<ul style="list-style-type: none"> • CO₂ pressure: 27.6 MPa • Temperature: 40 °C • Time: 153 min • Flow rate: 30 g/min 	<ul style="list-style-type: none"> • Ginger extract: 8.6% (ginger oleoresin: 38 wt.% and ginger oil: 28 wt.%) 	Shukla et al. [163]
Patè olive cake	<ul style="list-style-type: none"> • CO₂ pressure: 44 MPa • Temperature: 40 °C • Time: 30 min 	<ul style="list-style-type: none"> • Oil yield: 14.5 wt.% (phytosterols, tocopherol and squalene) 	Durante et al. [164]
<i>Pogostemon cablin</i> (Patchouli)	<ul style="list-style-type: none"> • CO₂ pressure: 20 MPa • Temperature: 80 °C • Time: 30 min 	<ul style="list-style-type: none"> • Crude extract: 12.4% (Patchouli alcohol: 37.4%, δ-guaiene: 20.3%, azulene: 17.2% and seychellene: 7.8%) • Patchouli oil: 7.7% 	Muhammad et al. [165]

Shukla et al. [163] conducted a study on the extraction of ginger oil and oleoresin from ginger rhizomes. This study delivered a total ginger extract of 8.6 wt.% with a high selectivity towards the extraction of ginger oleoresin (around 40%) at 40 °C and 28 MPa CO₂ pressure in 153 min. Ginger oleoresin has many applications in the food and pharmaceutical

industries. Patchouli, a flowering plant in the mint family, also has many value-added uses in the food, nutraceutical and pharmaceutical industries due to its terpene alcohol-based essential oil content. This essential oil has been extracted through SCCO₂ with a higher yield of azulene, patchouli alcohol and δ -guaiene [165].

In addition to the extraction of alcohol-based compounds, the widespread application of SCCO₂ is also found in the extraction of non-polar molecules such as fatty acids and lipids from various feedstock due to their non-polar nature. Leone et al. [158] performed SCCO₂ extraction of eicosapentaenoic acid and docosahexaenoic acid from microalgae *Nannochloropsis* sp. They observed the highest eicosapentaenoic acid yield of 5.6 mg/g and docosahexaenoic acid yield of 0.12 mg/g under a CO₂ pressure of 55 MPa (at 75 °C) and 40 MPa (at 50 °C), respectively, with a constant extraction time of 100 min. With different combinations of temperatures and CO₂ pressures, the selectivity of various constituent molecules differs.

Subcritical CO₂ is also used to extract volatile flavoring compounds such as terpenoids from different aromatic plants and dairy products such as clarified butter [161]. These terpenoids have a greater significance in the food processing and pharmaceutical industries. For instance, various volatile flavoring compounds such as δ -dodecaltone, δ -tetradecalctone and 3-ethyl-3-methyl heptane can be extracted from clarified butter using subcritical CO₂ with a CO₂ pressure and temperatures less than 10 MPa and 15 °C, respectively, due to the lower volatilization of these compounds [161]. These compounds can be encapsulated and used in the food industry as flavoring agents.

In addition to their extraction potential, subcritical and supercritical CO₂ can be used as the reaction medium to prepare various cosmeceutical formulations, isolate certain compounds from a crude extract, conduct different organic reactions and separate compounds from a heterogeneous mixture in supercritical fluid-based liquid chromatography [166]. The fractionation property of SCCO₂ is applied in the upgrading of bio-crude oil through esterification and decreasing the oxygenated compounds such as carboxylic acids and different types of alcohols [167]. Cui et al. [168] performed non-catalytic bio-oil upgrading using SCCO₂ at 80 °C under a CO₂ pressure of 28 MPa and a fractionation time of 3 h. This upgrading of bio-oil was facilitated by SCCO₂ esterification converting 87% of carboxylic acids into esters and simultaneously decreasing the moisture and volatile contents. This subsequently increased the stability and calorific value of the upgraded bio-oil. SCCO₂ is also applied for the hydraulic fracturing of shale [144], which can lead to the recycling of CO₂ largely emitted from petrochemical refineries [169].

5. Conclusions

There is a steady advancement in carbon capture, utilization and storage technologies to address the issues of climate change and global warming. On a commercial scale, pre-combustion and post-combustion technologies are found to be viable carbon-capturing methods. Various other techniques such as direct air capture, chemical looping combustion, and gasification and ionic liquid are also found to be promising techniques. Currently, chemical looping combustion and gasification, ionic liquids, and biological CO₂ fixation might not be considered the largescale industrial routes for carbon capture and storage. However, according to the Intergovernmental Panel on Climate Change and the recent literature, these technologies are gaining attention as emerging technologies due to their environmentally friendly nature, although they require significant research, development and demonstration to compete with the well-established technologies such as pre-combustion, post-combustion, oxy-fuels and direct air capture. The chemical looping gasification technology can also lead to the production of clean H₂ in addition to sequestering CO₂. Ionic liquid-based CO₂ absorbents are suitable for commercial carbon capture because of their cost-effectiveness, adjustable structure and high absorption capabilities. Commercially available amines are attractive for industrial CO₂-capturing applications because of their high absorption capacities.

CO₂ capturing technologies have advanced over the years, and their utilization in fuel synthesis, production of carbonates and different valuable chemicals is a significant development in mitigating the challenges caused by GHGs. CO₂ storage as calcium and magnesium carbonate is one of the efficient geological storage methods. CO₂ is also considered a potential raw material for the synthesis of highly valued platform chemicals such as olefins, methanol, dimethyl ether and formic acid. Moreover, the processing of harvested algae yields carbohydrates, lipids, bioactive compounds and proteins, making them a suitable feedstock for the manufacturing of medicinal products, biofuels and biochemicals as well as for biological fixation of CO₂ and treating wastewater. Finally, to achieve net-zero emissions by 2050, significant research and development are required in the effective capturing, storage and utilization of CO₂ from the atmosphere using sustainable, industrially feasible and cost-effective technologies.

Author Contributions: Conceptualization, J.P., B.R.P., F.P. and S.N.; validation, J.P., B.R.P., F.P. and S.N.; investigation, J.P., B.R.P., F.P. and S.N.; resources, A.K.D.; data curation, J.P., B.R.P., F.P. and S.N.; writing—original draft preparation, J.P., B.R.P., F.P. and S.N.; writing—review and editing, J.P., B.R.P., F.P., S.N. and A.K.D.; visualization, J.P., B.R.P., F.P. and S.N.; supervision, A.K.D.; project administration, A.K.D.; funding acquisition, A.K.D. All authors have read and agreed to the published version of the manuscript.

Funding: The authors would like to thank the Natural Sciences and Engineering Research Council of Canada (NSERC), the Canada Research Chairs (CRC) program, BioFuelNet Canada and the Agriculture and Agri-Food Canada (AAFC) program for funding this work.

Data Availability Statement: Not applicable.

Conflicts of Interest: The authors declare no conflict of interest.

References

1. Zeng, C.; Stringer, L.C.; Lv, T. The spatial spillover effect of fossil fuel energy trade on CO₂ emissions. *Energy* **2021**, *223*, 120038. [CrossRef]
2. Nanda, S.; Reddy, S.N.; Mitra, S.K.; Kozinski, J.A. The progressive routes for carbon capture and sequestration. *Energy Sci. Eng.* **2016**, *4*, 99–122. [CrossRef]
3. Liu, Y.; Tang, H.; Muhammad, A.; Huang, G. Emission mechanism and reduction countermeasures of agricultural greenhouse gases—A review. *Greenhouse Gas Sci. Technol.* **2019**, *9*, 160–174. [CrossRef]
4. Majumdar, A.; Deutch, J. Research opportunities for CO₂ utilization and negative emissions at the gigatonne scale. *Joule* **2018**, *2*, 805–809. [CrossRef]
5. Wei, X.; Manovic, V.; Hanak, D.P. Techno-economic assessment of coal- or biomass-fired oxy-combustion power plants with supercritical carbon dioxide cycle. *Energy Convers. Manag.* **2020**, *221*, 113143. [CrossRef]
6. Rapier, R. Fossil Fuels Still Supply 84 Percent of World Energy—And Other Eye Openers from BP’s Annual Review, Forbes. Available online: <https://www.forbes.com/sites/rrapier/2020/06/20/bp-review-new-highs-in-global-energy-consumption-and-carbon-emissions-in-2019/?sh=8dd42c166a16> (accessed on 24 August 2022).
7. National Oceanic & Atmospheric Administration (NOAA). Global Monitoring Laboratory. Trends in Atmospheric Carbon Dioxide. Available online: https://gml.noaa.gov/ccgg/trends/gl_trend.html (accessed on 16 January 2023).
8. Hale, I.; Hale, D.; Howard, C.; Bell, W. Time to divest from the fossil-fuel industry. *Can. Med. Assoc. J.* **2014**, *186*, 960.
9. Our World in Data. Why Do Greenhouse Gas Emissions Matter? Available online: <https://ourworldindata.org/co2-and-other-greenhouse-gas-emissions> (accessed on 28 July 2022).
10. NASA. Global Climate Change. The Effects of Climate Change. Available online: <https://climate.nasa.gov/effects/#:~:text=Climate%20change%20has%20caused%20increased,related%20health%20impacts%20in%20cities> (accessed on 25 August 2022).
11. Raza, A.; Gholami, R.; Rezaee, R.; Rasouli, V.; Rabiei, M. Significant aspects of carbon capture and storage—A review. *Petroleum* **2019**, *5*, 335–340.
12. COP26, United Nations Climate Change Conference 2022. Available online: <https://ukcop26.org/cop26-goals> (accessed on 24 August 2022).
13. United States Environmental Protection Agency (USEPA). Global Greenhouse Gas Emissions Data. Available online: <https://www.epa.gov/ghgemissions/global-greenhouse-gas-emissions-data> (accessed on 28 July 2022).
14. Gerlach, T. Volcanic versus anthropogenic carbon dioxide. *EOS* **2011**, *92*, 201. [CrossRef]
15. International Energy Agency (IEA). Global CO₂ Emissions Rebounded to Their Highest Level in History in 2021. Available online: <https://www.iea.org/news/global-co2-emissions-rebounded-to-their-highest-level-in-history-in-2021> (accessed on 25 August 2022).

16. Plaza, M.G.; Martínez, S.; Rubiera, F. CO₂ capture, use, and storage in the cement industry: State of the art and expectations. *Energies* **2020**, *13*, 5692. [CrossRef]
17. Fan, Z.; Friedmann, S.J. Low-carbon production of iron and steel: Technology options, economic assessment, and policy. *Joule* **2021**, *5*, 829–862.
18. Patra, B.R.; Gouda, S.P.; Pattnaik, F.; Nanda, S.; Dalai, A.K.; Naik, S. A brief overview of recent advancements in CO₂ capture and valorization technologies. In *Carbon Dioxide Capture and Conversion*; Nanda, S., Vo, D.V.N., Nguyen, V.H., Eds.; Elsevier: Amsterdam, The Netherlands, 2022; pp. 1–16.
19. Im, S.; Petersen, S.O.; Lee, D.; Kim, D.H. Effects of storage temperature on CH₄ emissions from cattle manure and subsequent biogas production potential. *Waste Manag.* **2020**, *101*, 35–43.
20. Patra, B.R.; Mukherjee, A.; Nanda, S.; Dalai, A.K. Biochar production, activation and adsorptive applications: A review. *Environ. Chem. Lett.* **2021**, *19*, 2237–2259.
21. Patra, B.R.; Nanda, S.; Dalai, A.K.; Meda, V. Taguchi-based process optimization for activation of agro-food waste biochar and performance test for dye adsorption. *Chemosphere* **2021**, *285*, 131531. [PubMed]
22. Jing, Y.; Rabbani, A.; Armstrong, R.T.; Wang, J.; Zhang, Y.; Mostaghimi, P. An image-based coal network model for simulating hydro-mechanical gas flow in coal: An application to carbon dioxide geo-sequestration. *J. Clean. Prod.* **2022**, *379*, 134647.
23. Aresta, M.; Dibenedetto, A.; Angelini, A. The changing paradigm in CO₂ utilization. *J. CO₂ Util.* **2013**, *3*, 65–73.
24. Shafawi, A.N.; Mohamed, A.R.; Lahijani, P.; Mohammadi, M. Recent advances in developing engineered biochar for CO₂ capture: An insight into the biochar modification approaches. *J. Environ. Chem. Eng.* **2021**, *9*, 106869.
25. Zhang, S.; Liu, Z. Advances in the biological fixation of carbon dioxide by microalgae. *J. Chem. Tech. Biotechnol.* **2021**, *96*, 1475–1495. [CrossRef]
26. Valluri, S.; Clarendon, V.; Kawatra, S. Opportunities and challenges in CO₂ utilization. *J. Environ. Sci.* **2022**, *113*, 322–344.
27. Intergovernmental Panel on Climate Change (IPCC). *Carbon Dioxide Capture and Storage*; Metz, B., Davidson, O., de Coninck, H., Loos, M., Meyer, L., Eds.; Cambridge University Press: Cambridge, UK, 2005; p. 431.
28. Zhou, T.; Shi, H.; Ding, X.; Zhou, Y. Thermodynamic modeling and rational design of ionic liquids for pre-combustion carbon capture. *Chem. Eng. Sci.* **2021**, *229*, 116076. [CrossRef]
29. Madejski, P.; Chmiel, K.; Subramanian, N.; Kuś, T. Methods and techniques for CO₂ capture: Review of potential solutions and applications in modern energy technologies. *Energies* **2022**, *15*, 887.
30. Portillo, E.; Alonso-Fariñas, B.; Vega, F.; Cano, M.; Navarrete, B. Alternatives for oxygen-selective membrane systems and their integration into the oxy-fuel combustion process: A review. *Sep. Purif. Technol.* **2019**, *229*, 115708. [CrossRef]
31. Dakota Gasification Company. Gasification. Available online: <https://www.dakotagas.com/about-us/gasification/index> (accessed on 17 February 2023).
32. Olabi, A.G.; Obaideen, K.; Elsaid, K.; Wilberforce, T.; Sayed, E.T.; Maghrabie, H.M.; Abdelkareem, M.A. Assessment of the pre-combustion carbon capture contribution into sustainable development goals SDGs using novel indicators. *Renew. Sustain. Energy Rev.* **2022**, *153*, 111710.
33. Dakota Gasification Company. Souris Valley Pipeline Ltd. Available online: <https://www.dakotagas.com/about-us/pipelines/souris-valley-pipeline> (accessed on 17 February 2023).
34. Petroleum Technology Research Centre. Weyburn-Midale: The IEAGHG Weyburn-Midale CO₂ Monitoring and Storage Project. Available online: <https://ptrc.ca/projects/past-projects/weyburn-midale> (accessed on 17 February 2023).
35. EnergyWire. The Kemper Project Just Collapsed. *What It Signifies for CCS*. Available online: <https://www.eenews.net/articles/the-kemper-project-just-collapsed-what-it-signifies-for-ccs/> (accessed on 17 February 2023).
36. Capital News Service. In Maryland, a Potential Future for Cleaner Coal. Available online: <https://cnsmaryland.org/2013/12/03/in-maryland-a-potential-future-for-cleaner-coal/> (accessed on 17 February 2023).
37. O-BASF/Linde. Carbon Capture, Storage and Utilisation Linde & BASF Team up to Innovate Carbon Capture. 2023. Available online: https://www.linde-engineering.com/en/images/Carbon-capture-storage-utilisation-Linde-BASF_tcm19-462558.pdf (accessed on 17 February 2023).
38. Linde Engineering. CO₂ Purification and Liquefaction Plant with Food Grade Quality in Manchester, UK. Available online: <https://www.linde-engineering.com/en/process-plants/co2-plants/references/index.html> (accessed on 17 February 2023).
39. National Energy Technology Laboratory. ExxonMobil, NREL Partnership to Expand Key NETL Research Programs. Available online: <https://netl.doe.gov/node/8777> (accessed on 17 February 2023).
40. Cision. NET Power Demonstration Plant Wins 2018 ADIPEC Breakthrough Technological Project of the Year. Available online: <https://www.prnewswire.com/news-releases/net-power-demonstration-plant-wins-2018-adipec-breakthrough-technological-project-of-the-year-300750163.html> (accessed on 17 February 2023).
41. González-Nicolás, A.; Cihan, A.; Petrusak, R.; Zhou, Q.; Trautz, R.; Riestenberg, D.; Godec, M.; Birkholzer, J.T. Pressure management via brine extraction in geological CO₂ storage: Adaptive optimization strategies under poorly characterized reservoir conditions. *Int. J. Greenhouse Gas Control* **2019**, *83*, 176–185. [CrossRef]
42. Chatterjee, S.; Huang, K.W. Unrealistic energy and materials requirement for direct air capture in deep mitigation pathways. *Nature Comm.* **2020**, *11*, 3287. [CrossRef]
43. Custelcean, R. Direct air capture of CO₂ using solvents. *Annu. Rev. Chem. Biomol. Eng.* **2022**, *13*, 217–234. [CrossRef] [PubMed]

44. Jiang, L.; Liu, W.; Wang, R.Q.; Gonzalez-Diaz, A.; Rojas-Michaga, M.F.; Michailos, S.; Pourkashanian, M.; Zhang, X.J.; Font-Palma, C. Sorption direct air capture with CO₂ utilization. *Prog. Energy Combust. Sci.* **2023**, *95*, 101069.
45. Sefidi, V.S.; Luis, P. Advanced amino acid-based technologies for CO₂ capture: A review. *Ind. Eng. Chem. Res.* **2019**, *58*, 20181–20194.
46. Shi, X.; Xiao, H.; Azarabadi, H.; Song, J.; Wu, X.; Chen, X.; Lackner, K.S. Sorbents for the direct capture of CO₂ from ambient air. *Angew. Chem. Int. Ed.* **2020**, *59*, 6984–7006. [[CrossRef](#)]
47. Freitas, R.A., Jr. *The Nanofactory Solution to Global Climate Change: Atmospheric Carbon Capture*; IMM Report No. 45, 2015; Institute for Molecular Manufacturing: Palo Alto, CA, USA, 2015.
48. Kiani, A.; Lejeune, M.; Li, C.; Patel, J.; Feron, P. Liquefied synthetic methane from ambient CO₂ and renewable H₂-A techno-economic study. *J. Nat. Gas Sci. Eng.* **2021**, *94*, 104079. [[CrossRef](#)]
49. Climeworks, A.G. Fight Climate Change with Direct Air Capture. Available online: <https://climeworks.com/> (accessed on 17 February 2023).
50. Wurzbacher, J.; Gebald, C.; Brunner, S.; Steinfeld, A. Heat and mass transfer of temperature-vacuum swing desorption for CO₂ capture from air. *Chem. Eng. J.* **2016**, *283*, 1329–1338. [[CrossRef](#)]
51. Beuttler, C.; Charles, L.; Wurzbacher, J. The role of direct air capture in mitigation of anthropogenic greenhouse gas emissions. *Front. Climate* **2019**, *1*, 10. [[CrossRef](#)]
52. Carbon Engineering Ltd. We Believe Humanity Can Solve Climate Change. Available online: <https://carbonengineering.com/> (accessed on 17 February 2023).
53. Global Thermostat. A Carbon Negative Solution. Available online: <https://globalthermostat.com/> (accessed on 17 February 2023).
54. National Air and Space Museum. Canister, Lithium Hydroxide, Command Module, Apollo 11. Available online: <https://airandspace.si.edu> (accessed on 29 November 2022).
55. Kim, J.Y.; Ellis, N.; Lim, C.J.; Grace, J.R. Effect of calcination/carbonation and oxidation/reduction on attrition of binary solid species in sorption-enhanced chemical looping reforming. *Fuel* **2020**, *271*, 117665. [[CrossRef](#)]
56. Abuelgasim, S.; Wang, W.; Abdalazeez, A. A brief review for chemical looping combustion as a promising CO₂ capture technology: Fundamentals and progress. *Sci. Total Environ.* **2021**, *764*, 142892. [[CrossRef](#)]
57. Farajollahi, H.; Hossainpour, S. Macroscopic model-based design and techno-economic assessment of a 300 MWth in-situ gasification chemical looping combustion plant for power generation and CO₂ capture. *Fuel Process. Technol.* **2022**, *231*, 107244. [[CrossRef](#)]
58. Zheng, S.; Zeng, S.; Li, Y.; Bai, L.; Bai, Y.; Zhang, X.; Liang, X.; Zhang, S. State of the art of ionic liquid-modified adsorbents for CO₂ capture and separation. *AIChE J.* **2022**, *68*, e17500. [[CrossRef](#)]
59. Gurkan, B.; Goodrich, B.F.; Mindrup, E.M.; Ficke, L.E.; Massel, M.; Seo, S.; Senftle, T.P.; Wu, H.; Glaser, M.F.; Shah, J.K.; et al. Molecular design of high capacity, low viscosity, chemically tunable ionic liquids for CO₂ capture. *J. Phys. Chem. Lett.* **2010**, *1*, 3494–3499. [[CrossRef](#)]
60. Vadillo, J.M.; Díaz-Sainz, G.; Gómez-Coma, L.; Garea, A.; Irabien, A. Chemical and physical ionic liquids in CO₂ capture system using membrane vacuum regeneration. *Membranes* **2022**, *12*, 785. [[CrossRef](#)] [[PubMed](#)]
61. Xia, S.M.; Chen, K.H.; Fu, H.C.; He, L.N. Ionic liquids catalysis for carbon dioxide conversion with nucleophiles. *Front. Chem.* **2018**, *6*, 462. [[CrossRef](#)]
62. Fu, H.C.; You, F.; Li, H.R.; He, L.N. CO₂ capture and in situ catalytic transformation. *Front Chem.* **2019**, *7*, 525. [[CrossRef](#)] [[PubMed](#)]
63. Gurkan, B.E.; de la Fuente, J.C.; Mindrup, E.M.; Ficke, L.E.; Goodrich, B.F.; Price, E.A. Equimolar CO₂ absorption by anion-functionalized ionic liquids. *J. Am. Chem. Soc.* **2010**, *132*, 2116–2117. [[CrossRef](#)]
64. Wang, C.M.; Luo, X.Y.; Luo, H.M.; Jiang, D.E.; Li, H.R.; Dai, S. Tuning the basicity of ionic liquids for equimolar CO₂ capture. *Angew. Chem. Int. Ed.* **2011**, *50*, 4918–4922. [[CrossRef](#)] [[PubMed](#)]
65. Wang, C.M.; Luo, H.M.; Li, H.R.; Zhu, X.; Yu, B.; Dai, S. Tuning the physicochemical properties of diverse phenolic ionic liquids for equimolar CO₂ capture by the substituent on the anion. *Chem.-Eur. J.* **2012**, *18*, 2153–2160. [[CrossRef](#)] [[PubMed](#)]
66. Boldoo, T.; Chinnasamy, V.; Kim, M.; Cho, H. CO₂ entrapment using 1-hexyl-3-methyl-imidazolium room temperature ionic liquids with multi-walled carbon nanotubes. *J. CO₂ Util.* **2022**, *66*, 102285. [[CrossRef](#)]
67. Luo, X.; Chen, K.; Li, H.; Wang, C. The capture and simultaneous fixation of CO₂ in the simulation of fuel gas by bifunctionalized ionic liquids. *Int. J. Hydrogen Energy.* **2016**, *41*, 9175–9182. [[CrossRef](#)]
68. Cantu, D.C.; Malhotra, D.; Koech, P.K.; Heldebrant, D.J.; Zheng, R.F.; Freeman, C.J.; Rousseau, R.; Glezakou, V.A. Integrated solvent design for CO₂ capture and viscosity tuning. *Energy Proc.* **2017**, *114*, 726–734. [[CrossRef](#)]
69. Costentin, C.; Drouet, S.; Robert, M.; Saveant, J.-M. A local proton source enhances CO₂ electroreduction to CO by a molecular Fe catalyst. *Science* **2012**, *338*, 90–94. [[CrossRef](#)]
70. Spinner, N.S.; Vega, J.A.; Mustain, W.E. Recent progress in the electrochemical conversion and utilization of CO₂. *Catal. Sci. Technol.* **2012**, *2*, 19–28. [[CrossRef](#)]
71. Ainsworth, E.A. Rice production in a changing climate: A meta-analysis of responses to elevated carbon dioxide and elevated ozone concentration. *Glob. Chang. Biol.* **2008**, *14*, 1642–1650. [[CrossRef](#)]
72. Ahmed, M.; Stöckle, C.O.; Nelson, R.; Higgins, S.; Ahmad, S.; Raza, M.A. Novel multimodel ensemble approach to evaluate the sole effect of elevated CO₂ on winter wheat productivity. *Sci. Rep.* **2019**, *9*, 7813. [[CrossRef](#)]
73. Mega, R.; Abe, F.; Kim, J.S.; Tsuboi, Y.; Tanaka, K.; Kobayashi, H.; Sakata, Y.; Hanada, K.; Tsujimoto, H.; Kikuchi, J.; et al. Tuning water-use efficiency and drought tolerance in wheat using abscisic acid receptors. *Nat. Plants* **2019**, *5*, 153–159. [[CrossRef](#)]

74. Kang, K.; Papari, S.; Bamdad, H.; Nanda, S.; Dalai, A.K.; Berruti, F. Algae as a bioresource for clean fuels, carbon fixation and wastewater reclamation. In *Algal Biorefinery: Developments, Challenges and Opportunities*; Dalai, A.K., Goud, V.V., Nanda, S., Borugadda, V.B., Eds.; Routledge: Abingdon, UK, 2021; pp. 1–23.
75. Yadav, P.; Reddy, S.N.; Nanda, S. Cultivation and conversion of algae for wastewater treatment and biofuel production. In *Fuel Processing and Energy Utilization*; Nanda, S., Sarangi, P.K., Vo, D.V.N., Eds.; CRC Press: Boca Raton, FL, USA, 2019; pp. 159–175.
76. Zhu, Z.; Jiang, J.; Fa, Y. Overcoming the biological contamination in microalgae and cyanobacteria mass cultivations for photosynthetic biofuel production. *Molecules* **2020**, *25*, 5220. [[CrossRef](#)] [[PubMed](#)]
77. Hans, N.; Pattnaik, F.; Malik, A.; Nanda, S.; Kumar, V.; Dalai, A.K.; Naik, S. Algal-derived physiologically active nutraceuticals: Dietary supplements, vitamins, carotenoids, fatty acids and other novel products. In *Algal Biorefinery: Developments, Challenges and Opportunities*; Dalai, A.K., Goud, V.V., Nanda, S., Borugadda, V.B., Eds.; Routledge: Abingdon, UK, 2021; pp. 197–230.
78. Burlacot, A.; Dao, O.; Auroy, P.; Cuiné, S.; Li-Beisson, Y.; Peltier, G. Alternative photosynthesis pathways drive the algal CO₂-concentrating mechanism. *Nature* **2022**, *605*, 366–371. [[CrossRef](#)]
79. Viswanaathan, S.; Perumal, P.K.; Sundaram, S. Integrated approach for carbon sequestration and wastewater treatment using algal–bacterial consortia: Opportunities and challenges. *Sustainability* **2022**, *14*, 1075. [[CrossRef](#)]
80. Jha, S.; Okolie, J.A.; Nanda, S.; Dalai, A.K. A review of biomass resources and thermochemical conversion technologies. *Chem. Eng. Technol.* **2022**, *45*, 791–799. [[CrossRef](#)]
81. Jha, S.; Nanda, S.; Acharya, B.; Dalai, A.K. A review of thermochemical conversion of waste biomass to biofuels. *Energies* **2022**, *15*, 6352. [[CrossRef](#)]
82. Napan, K.; Teng, L.; Quinn, J.C.; Wood, B.D. Impact of heavy metals from flue gas integration with microalgae production. *Algal Res.* **2015**, *8*, 83–88. [[CrossRef](#)]
83. Chou, H.H.; Su, H.Y.; Song, X.D.; Chow, T.J.; Chen, C.Y.; Chang, J.S.; Lee, T.M. Isolation and characterization of *Chlorella* sp. mutants with enhanced thermo- and CO₂ tolerances for CO₂ sequestration and utilization of flue gases. *Biotechnol. Biofuels* **2019**, *12*, 251. [[CrossRef](#)] [[PubMed](#)]
84. Nanda, S.; Dalai, A.K.; Berruti, F.; Kozinski, J.A. Biochar as an exceptional bioresource for energy, agronomy, carbon sequestration, activated carbon and specialty materials. *Waste Biomass Valor.* **2016**, *7*, 201–235. [[CrossRef](#)]
85. Masoumi, S.; Borugadda, V.B.; Nanda, S.; Dalai, A.K. Hydrochar: A review on its production technologies and applications. *Catalysts* **2021**, *11*, 939. [[CrossRef](#)]
86. Kang, K.; Nanda, S.; Hu, Y. Current trends in biochar application for catalytic conversion of biomass to biofuels. *Catal. Today* **2022**, *404*, 3–18. [[CrossRef](#)]
87. Zhao, X.; Liao, X.; He, L. The evaluation methods for CO₂ storage in coal beds in China. *J. Energy Inst.* **2016**, *89*, 389–399. [[CrossRef](#)]
88. Shabani, B.; Vilcáez, J. A fast and robust TOUGH2 module to simulate geological CO₂ storage in saline aquifers. *Comp. Geosci.* **2018**, *111*, 58–66. [[CrossRef](#)]
89. Chen, B.; Harp, D.R.; Lin, Y.; Keating, E.H.; Pawar, R.J. Geologic CO₂ sequestration monitoring design: A machine learning and uncertainty quantification based approach. *Appl. Energy* **2018**, *225*, 332–345. [[CrossRef](#)]
90. Koornneef, J.; Ramírez, A.; Turkenburg, W.; Faaij, A. The environmental impact and risk assessment of CO₂ capture, transport and storage—An evaluation of the knowledge base. *Prog. Energy Combust. Sci.* **2012**, *38*, 62–86. [[CrossRef](#)]
91. Agartan, E.; Gaddipati, M.; Yip, Y.; Savage, B.; Ozgen, C. CO₂ storage in depleted oil and gas fields in the Gulf of Mexico. *Int. J. Greenhouse Gas Cont.* **2018**, *72*, 38–48. [[CrossRef](#)]
92. Aminu, M.D.; Nabavi, S.A.; Rochelle, C.A.; Manovic, V. A review of developments in carbon dioxide storage. *Appl. Energy* **2017**, *208*, 1389–1419. [[CrossRef](#)]
93. Kumar, S.; Foroozesh, J.; Edlmann, K.; Rezk, M.G.; Lim, C.Y. A comprehensive review of value-added CO₂ sequestration in subsurface saline aquifers. *J. Nat. Gas Sci. Eng.* **2020**, *81*, 103437. [[CrossRef](#)]
94. Zhang, D.; Song, J. Mechanisms for geological carbon sequestration. *Proc. IUTAM* **2014**, *10*, 319–327. [[CrossRef](#)]
95. Reeves, S.; Taillefert, A.; Pekot, L.; Clarkson, C. *The Allison Unit CO₂-ECBM Pilot: A Reservoir Modeling Study*; Technical Report FC26-00NT40924; U.S. Department of Energy: Washington, DC, USA, 2003.
96. Zheng, S.; Yao, Y.; Elsworth, D.; Liu, D.; Cai, Y. Dynamic fluid interactions during CO₂-enhanced coalbed methane and CO₂ sequestration in coal seams. Part 1: CO₂–CH₄ interactions. *Energy Fuels* **2020**, *34*, 8274–8282. [[CrossRef](#)]
97. Ringrose, P.S.; Mathieson, A.S.; Wright, I.W.; Selama, F.; Hansen, O.; Bissell, R.; Saoula, N.; Midgley, J. The In Salah CO₂ storage project: Lessons learned and knowledge transfer. *Energy Proc.* **2013**, *37*, 6226–6236. [[CrossRef](#)]
98. Massachusetts Institute of Technology. Sleipner Fact Sheet: Carbon Dioxide Capture and Storage Project. Available online: <https://sequestration.mit.edu/tools/projects/sleipner.html> (accessed on 17 February 2023).
99. Yaashikaa, P.R.; Kumar, P.S.; Varjani, S.J.; Saravanan, A. A review on photochemical, biochemical and electrochemical transformation of CO₂ into value-added products. *J. CO₂ Util.* **2019**, *33*, 131–147. [[CrossRef](#)]
100. Okolie, J.A.; Patra, B.R.; Mukherjee, A.; Nanda, S.; Dalai, A.K.; Kozinski, J.A. Futuristic applications of hydrogen in energy, biorefining, aerospace, pharmaceuticals and metallurgy. *Int. J. Hydrog. Energy* **2021**, *46*, 8885–8905. [[CrossRef](#)]
101. Pattnaik, F.; Patra, B.R.; Okolie, J.A.; Nanda, S.; Dalai, A.K.; Naik, S. A review of thermocatalytic conversion of biogenic wastes into crude biofuels and biochemical precursors. *Fuel* **2022**, *320*, 123857. [[CrossRef](#)]
102. Lan, J.; Qu, Y.; Zhang, X.; Ma, H.; Xu, P.; Sun, J. A novel water-stable MOF Zn (Py)(Atz) as heterogeneous catalyst for chemical conversion of CO₂ with various epoxides under mild conditions. *J. CO₂ Util.* **2020**, *35*, 216–224. [[CrossRef](#)]

103. Liu, R.; Ma, Z.; Sears, J.D.; Juneau, M.; Neidig, M.L.; Porosoff, M.D. Identifying correlations in Fischer-Tropsch synthesis and CO₂ hydrogenation over Fe-based ZSM-5 catalysts. *J. CO₂ Util.* **2020**, *41*, 101290. [[CrossRef](#)]
104. Liu, R.; Leshchev, D.; Stavitski, E.; Juneau, M.; Agwara, J.N.; Porosoff, M.D. Selective hydrogenation of CO₂ and CO over potassium promoted Co/ZSM-5. *Appl. Catal. B Environ.* **2021**, *284*, 119787. [[CrossRef](#)]
105. Juneau, M.; Pope, C.; Liu, R.; Porosoff, M.D. Support acidity as a descriptor for reverse water-gas shift over Mo₂C-based catalysts. *Appl. Catal. A Gen.* **2021**, *620*, 118034. [[CrossRef](#)]
106. Juneau, M.; Yaffe, D.; Liu, R.; Agwara, J.N.; Porosoff, M.D. Establishing tungsten carbides as active catalysts for CO₂ hydrogenation. *Nanoscale* **2022**, *14*, 16458–16466. [[CrossRef](#)]
107. Liu, R.; El Berch, J.N.; House, S.; Meil, S.W.; Mpourmpakis, G.; Porosoff, M.D. Reactive separations of CO/CO₂ mixtures over Ru–Co single atom alloys. *ACS Catal.* **2023**, *13*, 2449–2461. [[CrossRef](#)]
108. Xu, D.; Hong, X.; Liu, G. Highly dispersed metal doping to ZnZr oxide catalyst for CO₂ hydrogenation to methanol: Insight into hydrogen spillover. *J. Catal.* **2021**, *393*, 207–214. [[CrossRef](#)]
109. Lan, J.; Qu, Y.; Xu, P.; Sun, J. Novel HBD-Containing Zn (dobdc)(datz) as efficiently heterogeneous catalyst for CO₂ chemical conversion under mild conditions. *Green Energy Environ.* **2021**, *6*, 66–74. [[CrossRef](#)]
110. Krishnan, J.U.; Jakka, S.C.B. TiO₂ nanorod supported multi-metallic heterogeneous catalyst for conversion of CO₂ to methanol under moderate operating conditions. *Inorg. Chem. Commun.* **2022**, *139*, 109375. [[CrossRef](#)]
111. Bankar, B.D.; Naikwadi, D.R.; Tayade, R.J.; Biradar, A.V. Direct hydrogenation of CO₂ to formic acid using Ru supported Co₃O₄ oxide as an efficient heterogeneous catalyst. *Mol. Catal.* **2023**, *535*, 112875. [[CrossRef](#)]
112. Hatsukade, T.; Kuhl, K.P.; Cave, E.R.; Abram, D.N.; Jaramillo, T.F. Insights into the electrocatalytic reduction of CO₂ on metallic silver surfaces. *Phys. Chem. Chem. Phys.* **2014**, *16*, 13814–13819. [[CrossRef](#)]
113. Yang, H.; Kaczur, J.J.; Sajjad, S.D.; Masel, R.I. CO₂ conversion to formic acid in a three compartment cell with Sustainion™ membranes. *ECS Trans* **2017**, *77*, 1425. [[CrossRef](#)]
114. Tan, X.; Yu, C.; Zhao, C.; Huang, H.; Yao, X.; Han, X.; Guo, W.; Cui, S.; Huang, H.; Qiu, J. Restructuring of Cu₂O to Cu₂O@Cu-metal–organic frameworks for selective electrochemical reduction of CO₂. *ACS Appl. Mater. Interfaces* **2019**, *11*, 9904–9910. [[CrossRef](#)] [[PubMed](#)]
115. Wang, L.; Peng, H.; Lamaison, S.; Qi, Z.; Koshy, D.M.; Stevens, M.B.; Wakerley, D.; Zeledón, J.A.Z.; King, L.A.; Zhou, L.; et al. Bimetallic effects on Zn-Cu electrocatalysts enhance activity and selectivity for the conversion of CO₂ to CO. *Chem. Catal.* **2021**, *1*, 663–680. [[CrossRef](#)]
116. Xie, Q.; Larrazábal, G.O.; Ma, M.; Chorkendorff, I.; Seger, B.; Luo, J. Copper-indium hydroxides derived electrocatalysts with tunable compositions for electrochemical CO₂ reduction. *J. Energy Chem.* **2021**, *63*, 278–284. [[CrossRef](#)]
117. Di, T.; Zhu, B.; Cheng, B.; Yu, J.; Xu, J. A direct Z-scheme g-C₃N₄/SnS₂ photocatalyst with superior visible-light CO₂ reduction performance. *J. Catal.* **2017**, *352*, 532–541. [[CrossRef](#)]
118. Shown, I.; Samireddi, S.; Chang, Y.C.; Putikam, R.; Chang, P.H.; Sabbah, A.; Fu, W.F.; Wu, C.I.; Yu, T.Y.; Chung, P.W.; et al. Carbon-doped SnS₂ nanostructure as a high-efficiency solar fuel catalyst under visible light. *Nat. Commun.* **2018**, *9*, 169. [[CrossRef](#)]
119. Kumar, P.; Joshi, C.; Barras, A.; Sieber, B.; Addad, A.; Boussekey, L.; Szuneritis, S.; Boukherroub, R.; Jain, S.L. Core-shell structured reduced graphene oxide wrapped magnetically separable rGO@CuZnO@Fe₃O₄ microspheres as superior photocatalyst for CO₂ reduction under visible light. *Appl. Catal. B Environ.* **2017**, *205*, 654–665. [[CrossRef](#)]
120. Wang, H.; Zhang, L.; Wang, K.; Sun, X.; Wang, W. Enhanced photocatalytic CO₂ reduction to methane over WO₃·0.33 H₂O via Mo doping. *Appl. Catal. B Environ.* **2019**, *243*, 771–779. [[CrossRef](#)]
121. Wang, W.; Deng, C.; Xie, S.; Li, Y.; Zhang, W.; Sheng, H.; Chen, C.; Zhao, J. Photocatalytic C–C coupling from carbon dioxide reduction on copper oxide with mixed-valence copper (I)/copper (II). *J. Am. Chem. Soc.* **2021**, *143*, 2984–2993. [[CrossRef](#)] [[PubMed](#)]
122. Long, D.; Liu, J.; Bai, L.; Yan, L.; Liu, H.; Feng, Z.; Zheng, L.L.; Chen, X.; Li, S.; Lu, M. Continuously selective photocatalytic CO₂ fixation via controllable S/Se ratio in a TiO₂–MoS_xSe_y dual-excitation heterostructured nanotree. *ACS Photonics* **2020**, *7*, 3394–3400. [[CrossRef](#)]
123. Li, Y.; Wen, L.; Tan, T.; Lv, Y. Sequential co-immobilization of enzymes in metal-organic frameworks for efficient biocatalytic conversion of adsorbed CO₂ to formate. *Front. Bioeng. Biotechnol.* **2019**, *7*, 394. [[CrossRef](#)]
124. Kusakabe, T.; Tatsuke, T.; Tsuruno, K.; Hirokawa, Y.; Atsumi, S.; Liao, J.C.; Hanai, T. Engineering a synthetic pathway in cyanobacteria for isopropanol production directly from carbon dioxide and light. *Metab. Eng.* **2013**, *20*, 101–108. [[CrossRef](#)]
125. Xiong, W.; Morgan, J.A.; Ungerer, J.; Wang, B.; Maness, P.C.; Yu, J. The plasticity of cyanobacterial metabolism supports direct CO₂ conversion to ethylene. *Nat. Plants* **2015**, *1*, 15053. [[CrossRef](#)]
126. Bai, S.T.; De Smet, G.; Liao, Y.; Sun, R.; Zhou, C.; Beller, M.; Maes, B.U.W.; Sels, B.F. Homogeneous and heterogeneous catalysts for hydrogenation of CO₂ to methanol under mild conditions. *Chem. Soc. Rev.* **2021**, *50*, 4259–4298. [[CrossRef](#)]
127. Fan, F.; Liu, H.; Shao, S.; Gong, Y.; Gong, Y.; Li, G.; Tang, Z. Cobalt catalysts enable selective hydrogenation of CO₂ toward diverse products: Recent progress and perspective. *J. Phys. Chem. Lett.* **2021**, *12*, 10486–10496. [[CrossRef](#)]
128. Liang, C.; Hu, X.; Wei, T.; Jia, P.; Zhang, Z.; Dong, D.; Zhang, S.; Liu, Q.; Hu, G. Methanation of CO₂ over Ni/Al₂O₃ modified with alkaline earth metals: Impacts of oxygen vacancies on catalytic activity. *Int. J. Hydrogen Energy* **2019**, *44*, 8197–8213. [[CrossRef](#)]
129. le Saché, E.; Reina, T.R. Analysis of dry reforming as direct route for gas phase CO₂ conversion. The past, the present and future of catalytic DRM technologies. *Prog. Energy Combust. Sci.* **2022**, *89*, 100970. [[CrossRef](#)]

130. Zhang, Q.; Bown, M.; Pastor-Pérez, L.; Duyar, M.S.; Reina, T.R. CO₂ conversion via reverse water gas shift reaction using fully selective Mo–P multicomponent catalysts. *Ind. Eng. Chem. Res.* **2022**, *61*, 12857–12865. [CrossRef]
131. Perathoner, S.; Centi, G. CO₂ recycling: A key strategy to introduce green energy in the chemical production chain. *ChemSusChem*. **2014**, *7*, 12741282. [CrossRef] [PubMed]
132. Xie, J.; Paalanen, P.P.; van Deelen, T.W.; Weckhuysen, B.M.; Louwerse, M.J.; de Jong, K.P. Promoted cobalt metal catalysts suitable for the production of lower olefins from natural gas. *Nat. Comm.* **2019**, *10*, 167. [CrossRef]
133. Martín, M.; Grossmann, I.E. Towards zero CO₂ emissions in the production of methanol from switchgrass. CO₂ to methanol. *Comput. Chem. Eng.* **2017**, *105*, 308–316. [CrossRef]
134. González-Tenorio, D.; Muñoz-Páez, K.M.; Valdez-Vazquez, I. Butanol production coupled with acidogenesis and CO₂ conversion for improved carbon utilization. *Biomass Convers. Biorefin.* **2022**, *12*, 2121–2131. [CrossRef]
135. Morales-Guio, C.G.; Cave, E.R.; Nitopi, S.A.; Feaster, J.T.; Wang, L.; Kuhl, K.P.; Jackson, A.; Johnson, N.C.; Abram, D.N.; Hatsukade, T.; et al. Improved CO₂ reduction activity towards C₂₊ alcohols on a tandem gold on copper electrocatalyst. *Nature Catal.* **2018**, *1*, 764–771. [CrossRef]
136. Ding, P.; Zhao, H.; Li, T.; Luo, Y.; Fan, G.; Chen, G.; Gao, S.; Shi, X.; Lu, S.; Sun, X. Metal-based electrocatalytic conversion of CO₂ to formic acid/formate. *J. Mater. Chem.* **2020**, *8*, 21947–21960. [CrossRef]
137. Yang, X.; Wu, S.; Zhang, Q.; Qiu, S.; Wang, Y.; Tan, J.; Ma, L.; Wang, T.; Xia, Y. Surface structure engineering of PdAg alloys with boosted CO₂ electrochemical reduction performance. *Nanomaterials* **2022**, *12*, 3860. [CrossRef] [PubMed]
138. Chaugule, A.A.; Tamboli, A.H.; Kim, H. Ionic liquid as a catalyst for utilization of carbon dioxide to production of linear and cyclic carbonate. *Fuel* **2017**, *200*, 316–332. [CrossRef]
139. Chang, R.; Choi, D.; Kim, M.H.; Park, Y. Tuning crystal polymorphisms and structural investigation of precipitated calcium carbonates for CO₂ mineralization. *ACS Sustain. Chem. Eng.* **2017**, *5*, 1659–1667. [CrossRef]
140. Aresta, M.; Dibenedetto, A.; Angelini, A. Catalysis for the valorization of exhaust carbon: From CO₂ to chemicals, materials, and fuels. Technological use of CO₂. *Chem. Rev.* **2014**, *114*, 1709–1742. [CrossRef] [PubMed]
141. Fukuoka, S.; Fukawa, I.; Adachi, T.; Fujita, H.; Sugiyama, N.; Sawa, T. industrialization and expansion of green sustainable chemical process: A review of non-phosgene polycarbonate from CO₂. *Org. Process Res. Dev.* **2019**, *23*, 145–169. [CrossRef]
142. Niaounakis, M. *Biopolymers: Applications and Trends*, 1st ed.; William Andrew: Oxford, UK, 2015; pp. 1–559.
143. Pattnaik, F.; Hans, N.; Patra, B.R.; Nanda, S.; Kumar, V.; Naik, S.N.; Dalai, A.K. Valorization of wild-type *Cannabis indica* by supercritical CO₂ extraction and insights into the utilization of raffinate biomass. *Molecules* **2023**, *28*, 207. [CrossRef]
144. Zhang, X.; Zhu, W.; Xu, Z.; Liu, S.; Wei, C. A review of experimental apparatus for supercritical CO₂ fracturing of shale. *J. Petrol. Sci. Eng.* **2022**, *208*, 109515. [CrossRef]
145. Su, R.; Yu, Z.; Xia, L.; Sun, J. Performance analysis and multi-objective optimization of an integrated gas turbine/supercritical CO₂ recompression/transcritical CO₂ cogeneration system using liquefied natural gas cold energy. *Energy Convers. Manag.* **2020**, *220*, 113136. [CrossRef]
146. Pattnaik, F.; Nanda, S.; Mohanty, S.; Dalai, A.K.; Kumar, V.; Ponnusamy, S.K.; Naik, S. *Cannabis: Chemistry, extraction and therapeutic applications*. *Chemosphere* **2022**, *289*, 133012. [CrossRef] [PubMed]
147. Ahn, Y.; Bae, S.J.; Kim, M.; Cho, S.K.; Baik, S.; Lee, J.I.; Cha, J.E. Review of supercritical CO₂ power cycle technology and current status of research and development. *Nuclear Eng. Technol.* **2015**, *47*, 647–661. [CrossRef]
148. Advanced Science News. Electrochemical Carbon Dioxide Reduction in Supercritical Carbon Dioxide is Cool. Available online: <https://www.advancedsciencenews.com/electrochemical-carbon-dioxide-reduction-in-supercritical-carbon-dioxide-is-cool/> (accessed on 16 February 2023).
149. Melchaeva, O.; Voyame, P.; Bassetto, V.C.; Prokein, M.; Renner, M.; Weidner, E.; Petermann, M.; Battistel, A. Electrochemical reduction of protic supercritical CO₂ on copper electrodes. *ChemSusChem* **2017**, *10*, 3660–3670. [CrossRef]
150. Jiménez, C.; García, J.; Martínez, F.; Camarillo, R.; Rincón, J. Deposition of Cu on CNT to synthesize electrocatalysts for the electrochemical reduction of CO₂: Advantages of supercritical fluid deposition technique. *J. Supercrit. Fluids* **2020**, *166*, 104999. [CrossRef]
151. Puring, K.J.; Evers, O.; Prokein, M.; Siegmund, D.; Scholten, F.; Mölders, N.; Renner, M.; Cuenya, B.R.; Petermann, M.; Weidner, E.; et al. Assessing the influence of supercritical carbon dioxide on the electrochemical reduction to formic acid using carbon-supported copper catalysts. *ACS Catal.* **2020**, *10*, 12783–12789. [CrossRef]
152. Liu, B.; Shi, J.; Wang, M.; Zhang, J.; Sun, B.; Shen, Y.; Sun, X. Reduction in interfacial tension of water–oil interface by supercritical CO₂ in enhanced oil recovery processes studied with molecular dynamics simulation. *J. Supercrit. Fluids* **2016**, *111*, 171–178. [CrossRef]
153. Li, L.; Zhou, X.; Su, Y.; Xiao, P.; Cui, M.; Zheng, J. Potential and challenges for the new method supercritical CO₂/H₂O mixed fluid huff-n-puff in shale oil EOR. *Front. Energy Res.* **2022**, *10*, 1041851. [CrossRef]
154. Djimasbe, R.; Varfolomeev, M.A.; Al-muntaser, A.A.; Yuan, C.; Suwaid, M.A.; Feoktistov, D.A.; Rakhmatullin, I.Z.; Milovankin, A.A.; Murzakhonov, F.; Morozov, V.; et al. Deep insights into heavy oil upgrading using supercritical water by a comprehensive analysis of GC, GC–MS, NMR, and SEM–EDX with the aid of EPR as a complementary technical analysis. *ACS Omega* **2021**, *6*, 135–147. [CrossRef] [PubMed]
155. McMahon, J. NET Power CEO Announces Four New Zero-Emission Gas Plants Underway. *Forbes*. Available online: <https://www.forbes.com/sites/jeffmcmahon/2021/01/08/net-power-ceo-announces-four-new-zero-emission-gas-plants-underway/?sh=2c4d6060175b> (accessed on 16 February 2023).

156. AirLiquide. Supercritical CO₂: Cleaner, Safer and More Competitive. Available online: <https://www.airliquide.com/stories/industry/supercritical-co2-cleaner-safer-and-more-competitive> (accessed on 16 February 2023).
157. Okolie, J.A.; Nanda, S.; Dalai, A.K.; Kozinski, J.A. Advances in the industrial applications of supercritical carbon dioxide. In *Carbon Dioxide Capture and Conversion*; Nanda, S., Vo, D.V.N., Nguyen, V.H., Eds.; Elsevier: Amsterdam, The Netherlands, 2022; pp. 237–256.
158. Leone, G.P.; Balducci, R.; Mehariya, S.; Martino, M.; Larocca, V.; Di Sanzo, G.; Lovine, A.; Casella, P.; Marino, T.; Karatza, D.; et al. Selective extraction of ω -3 fatty acids from *Nannochloropsis* sp. using supercritical CO₂ extraction. *Molecules* **2019**, *24*, 2406. [[CrossRef](#)]
159. Salinas, F.; Vardanega, R.; Espinosa-Álvarez, C.; Jimenez, D.; Munoz, W.B.; Ruiz-Domínguez, M.C.; Meireles, M.A.A.; Cerezal-Mezquita, P. Supercritical fluid extraction of chañar (*Geoffroea decorticans*) almond oil: Global yield, kinetics and oil characterization. *J. Supercrit. Fluids* **2020**, *161*, 104824. [[CrossRef](#)]
160. Dimić, I.; Pavlić, B.; Rakita, S.; Cvetanović Kljakić, A.; Zeković, Z.; Teslić, N. Isolation of cherry seed oil using conventional techniques and supercritical fluid extraction. *Foods* **2022**, *12*, 11. [[CrossRef](#)]
161. Duhan, N.; Sahu, J.K.; Naik, S.N. Sub-critical CO₂ extraction of volatile flavour compounds from ghee and optimization of process parameters using response surface methodology. *LWT* **2020**, *118*, 108731. [[CrossRef](#)]
162. Gan, Y.; Xu, D.; Zhang, J.; Wang, Z.; Wang, S.; Guo, H.; Zhang, K.; Li, Y.; Wang, Y. *Rana chensinensis* ovum oil based on CO₂ supercritical fluid extraction: Response surface methodology optimization and unsaturated fatty acid ingredient analysis. *Molecules* **2020**, *25*, 4170. [[CrossRef](#)] [[PubMed](#)]
163. Shukla, A.; Naik, S.N.; Goud, V.V.; Das, C. Supercritical CO₂ extraction and online fractionation of dry ginger for production of high-quality volatile oil and gingerols enriched oleoresin. *Ind. Crops Prod.* **2019**, *130*, 352–362. [[CrossRef](#)]
164. Durante, M.; Ferramosca, A.; Treppiccione, L.; Di Giacomo, M.; Zara, V.; Montefusco, A.; Piro, G.; Mita, G.; Bergamo, P.; Lenucci, M.S. Application of response surface methodology (RSM) for the optimization of supercritical CO₂ extraction of oil from patè olive cake: Yield, content of bioactive molecules and biological effects in vivo. *Food Chem.* **2020**, *332*, 127405. [[CrossRef](#)]
165. Muhammad, S.; HPS, A.K.; Abd Hamid, S.; Danish, M.; Marwan, M.; Yunardi, Y.; Abdullah, C.K.; Faisal, F.; Yahya, E.B. Characterization of bioactive compounds from Patchouli extracted via supercritical carbon dioxide (SC-CO₂) extraction. *Molecules* **2022**, *27*, 6025. [[CrossRef](#)]
166. Manjare, S.D.; Dhingra, K. Supercritical fluids in separation and purification: A review. *Mater. Sci. Energy Technol.* **2019**, *2*, 463–484. [[CrossRef](#)]
167. Nanda, S.; Pattnaik, F.; Borugadda, V.B.; Dalai, A.K.; Kozinski, J.A.; Naik, S. Catalytic and noncatalytic upgrading of bio-oil to synthetic fuels: An introductory review. In *Catalytic and Noncatalytic Upgrading of Oils*; Dalai, A.K., Dadyburjor, D.B., Zheng, Y., Duan, A., Roberts, W.L., Nanda, S., Eds.; ACS Publications: Washington, DC, USA, 2021; Volume 1379, pp. 1–28.
168. Cui, H.Y.; Wang, J.H.; Zhuo, S.P.; Li, Z.H.; Wang, L.H.; Yi, W.M. Upgrading bio-oil by esterification under supercritical CO₂ conditions. *J. Fuel Chem. Technol.* **2010**, *38*, 673–678. [[CrossRef](#)]
169. Wang, H.; Liu, Y.; Laaksonen, A.; Krook-Riekkola, A.; Yang, Z.; Lu, X.; Ji, X. Carbon recycling—An immense resource and key to a smart climate engineering: A survey of technologies, cost and impurity impact. *Renew. Sustain. Energy Rev.* **2020**, *131*, 110010. [[CrossRef](#)]

Disclaimer/Publisher’s Note: The statements, opinions and data contained in all publications are solely those of the individual author(s) and contributor(s) and not of MDPI and/or the editor(s). MDPI and/or the editor(s) disclaim responsibility for any injury to people or property resulting from any ideas, methods, instructions or products referred to in the content.